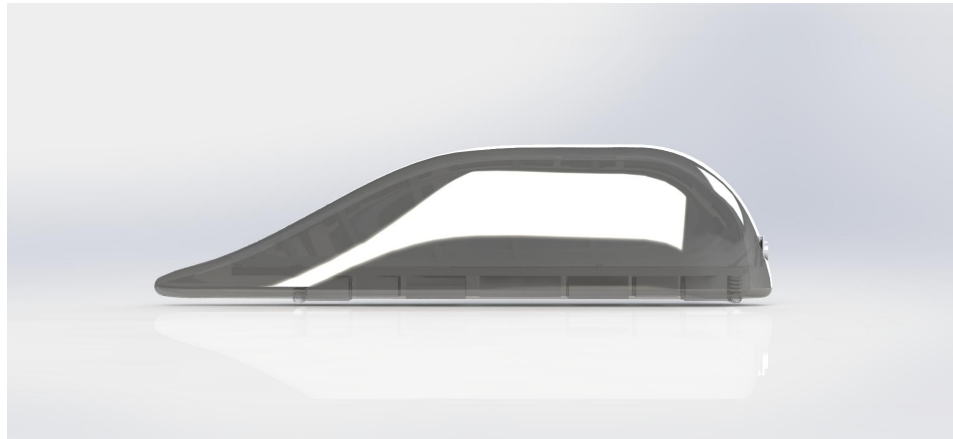


FLUXOR

Team Introduction

Fluxor is a continuation from OpenLoop SpaceX HyperLoop Round I, comprised of 18 Princeton University students. The team consists of students from a multitude of both concentrations and years, from computer science to mechanical engineering to political science. From our developments for the PDR, we have made significant progress towards making the finalized design described in the proposal captured herein. Much of our focus was on developing physical testing apparatuses for performing proof of concept testing (for magnet systems) and refining the details of controls/braking from the original design along with refining properties of the overall shell and chassis. In this presentation we will be discussing the following:

- Fuselage
- Suspension
- Braking
- Chassis
- Controls
- Competition Weekend



Team Members and Advisors



Team Members

Yash Patel (Leader)	Jonathan Jow
Daniel Chae	Max Becker
Francis Ogoke	Michael Lin
Juan Sepulveda	Nina Arcot
Stuart Pomeroy	Peter Russell
Arsh Dilbagi	Preeti Iyer
Ajay Penmatcha	Robert Cohen
Andrew Wang	Taylor Kulp-McDowall
Changxiao Xie	Henry Ha

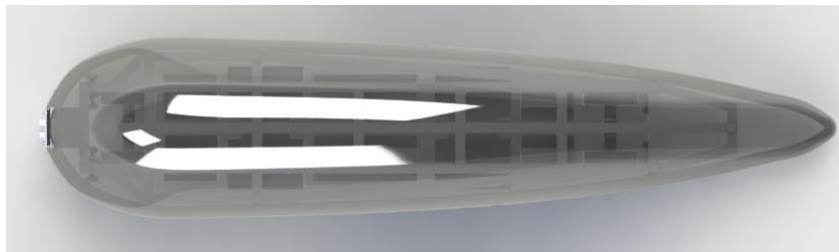


Advisors

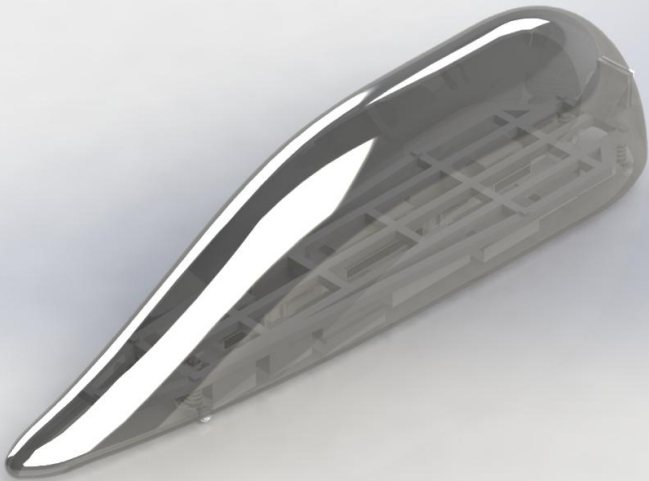
Professor Paul Cuff
Professor Glenn Northey
Al Gaillard

Top-Level Summary

The Fluxor pod is 13.2' x 3.3' x 3.3', with a unique duck-billed aerodynamic shell profile. The profile achieves minimal drag at the expected speeds we will attain and also ensures no shockwaves form in the regions above and below the pod. On the operational front pod, the Fluxor pod relies on magnetic suspension in the proven form of Halbach arrays, for which we have added further proof from internal testing. In particular, there will be four lifting Halbach arrays, each consisting of ten magnets (two sets of Halbach arrays), which are together capable of lifting the pod an expected 1.5 cm above the ground. Prior to liftoff, the pod will ride on a system of auxiliary wheels with springs. For sake of efficiency in build and simplicity, we will be using a similar system of magnets to achieve our regular braking, deployed with linear actuators. These are also coupled with a fail-safe emergency-brake, which is capable of singly braking the pod from top speed to rest in 10 seconds. If necessary, the pod can also actively deploy the emergency brake in conjunction with the regular braking system. These are both controlled through a system of Raspberry Pis, using error-correcting values determined through a Kalman Filter algorithm, all of which will be programmed with Python. These sensors will also be used for diagnostics of onboard system.



Final Design

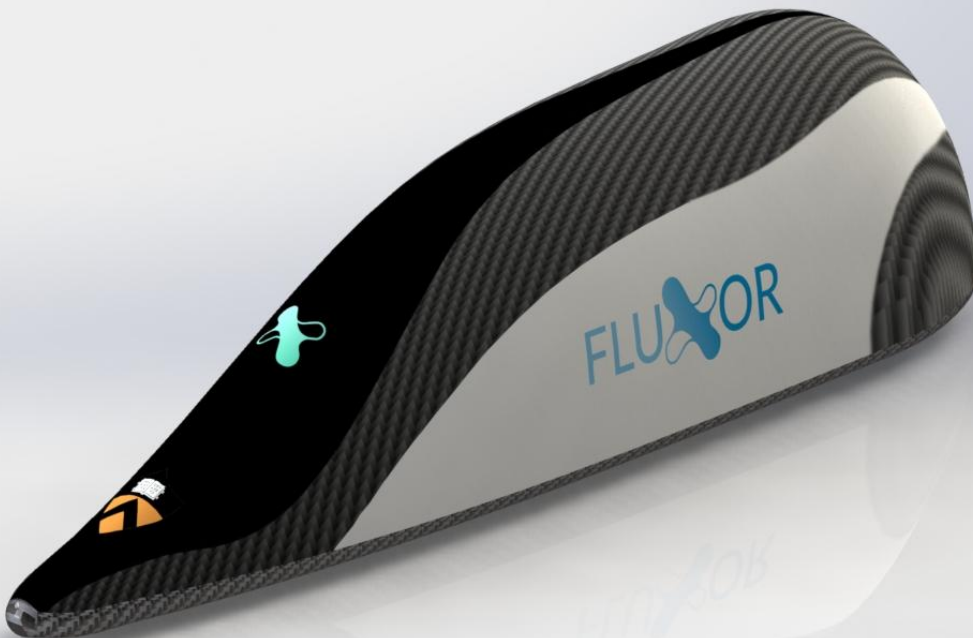


Overview

Below are overall breakdowns of the materials, cost, and mass, with more in-depth breakdowns provided in the corresponding sections and **Appendix A**:

Subsystem	Cost (\$)	Mass (kg)	Materials
Aerodynamic Shell	12,500	60	Carbon fiber
Suspension	4,250	45	Neodymium Magnets, Springs, Aluminum 7075
Braking (Regular & Emergency)	8,140	120	Nd Magnets, Aluminum 7075, Motors, Linear Actuators
Chassis	2,930	106	Aluminum 6061
Controls	1600	1.6	Raspberry Pis, Sensors, Batteries, Wires
Total	29,420	332.6	N/a

FUSELAGE



FLUXOR

Fuselage - System Overview

The direct goals of the fuselage are to:

- Provide a sleek, aerodynamic exterior to house the internals of the design, particularly the sensors and chassis. This “abstraction layer” gives the impression of a refined, safe transportation system, making moving at near Mach 1 significantly less frightening for the passengers.
- Maximize the ratio of pod volume to number of comfortably-housable passengers, assuming the passengers are typical human adults.

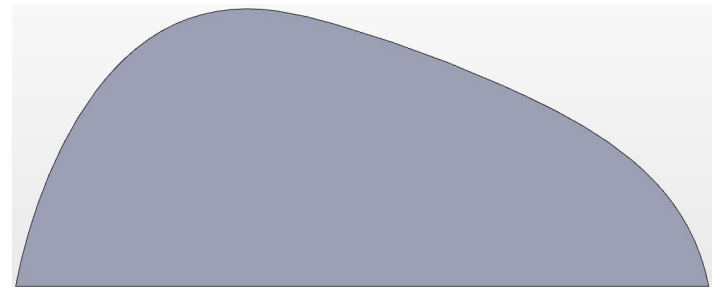
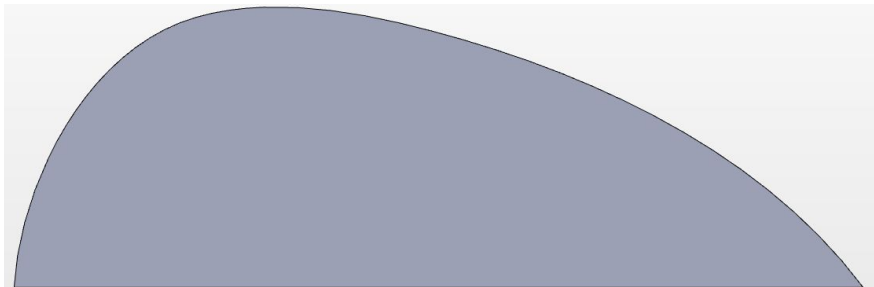
Applying these goals, our fuselage/pod has the following properties:

- Systems of neodymium magnets arranged as Halbach arrays, partially mounted parallel to the aluminum tracks and partially perpendicular, to provide respectively a 1.5 cm air gap and lateral stability.
- A simple system of linear actuators incorporated into the braking system, built on the principle of Eddy braking
- Max velocity of 128.5 m/s, or 287.4 mph
- Complete mass of 60 kg
- The empty, unused space of the pod, primarily towards the rear, will be allocated to carrying passengers.

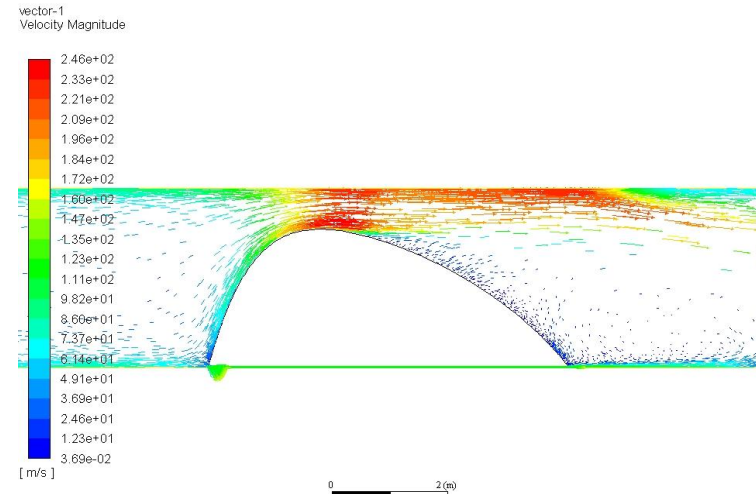
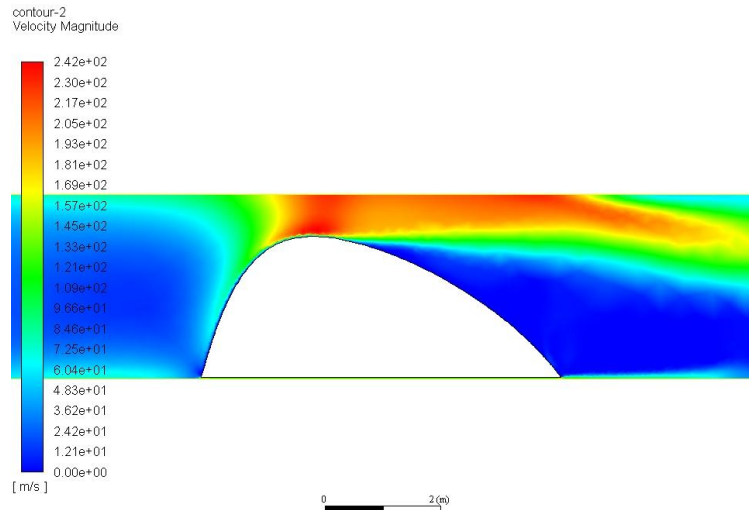
Fuselage - 2D CFD Setup

- Parameters of CFD simulation, including:
 - Freestream pressure: 100 Pa
 - Size of the CFD mesh: **165,985** cells (final version)
 - Size of the tube in CFD: 12x pod length (50m)
 - Time stepping algorithm used in simulation: Density-based SST k-omega model
 - Boundary conditions used for simulation:
 - Pressure far-field for the tube inlet and outlet
 - Symmetry BC used for the wall, and wall BC used for the pod itself

There were several profiles that were tested, of the varieties below. We only include the results of iterations that had very distinct profiles or exhibited significant improvement.

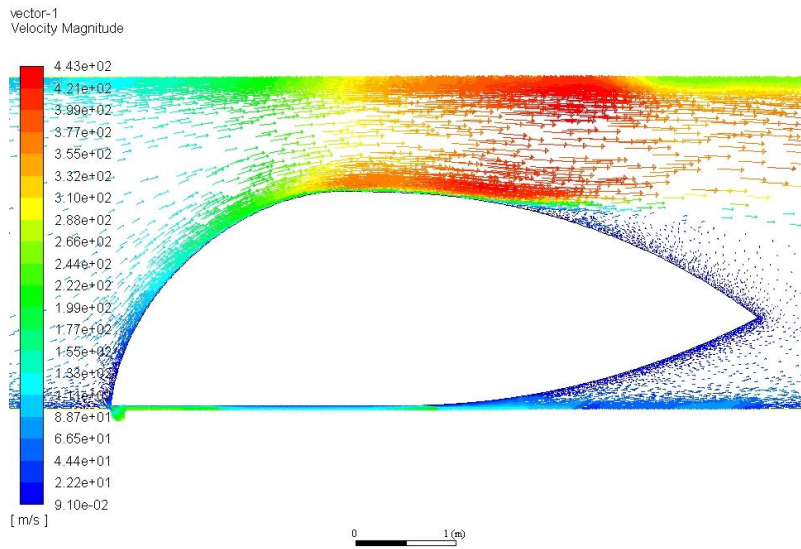
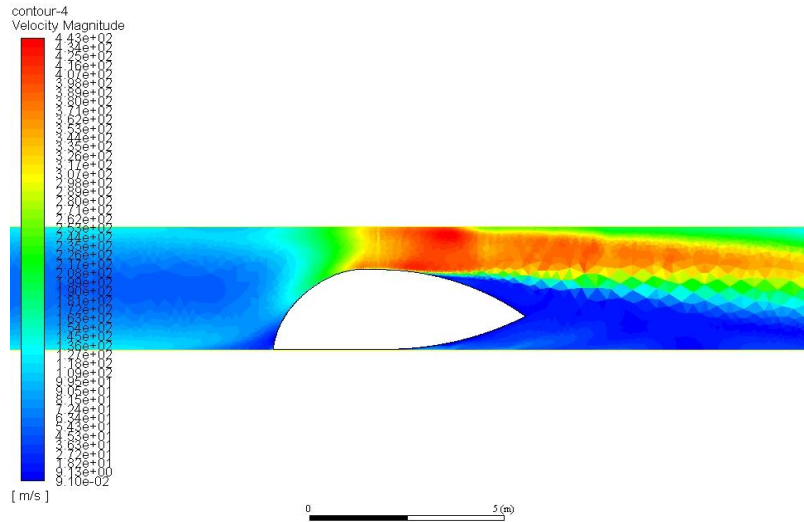


Fuselage - 2D CFD Results: Standard Design (120 m/s)



Drag: 95 N
Max air velocity: 242 m/s
Max Turbulent Kinetic Energy: 4057 m² /s²

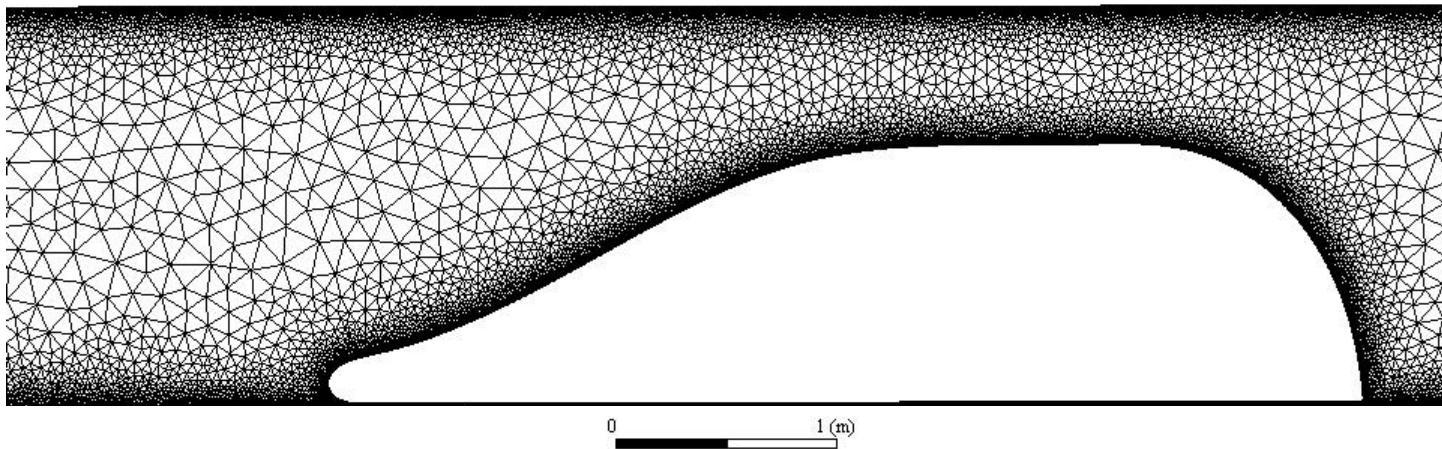
Fuselage - 2D CFD Results: Tail-Up Design (120 m/s)



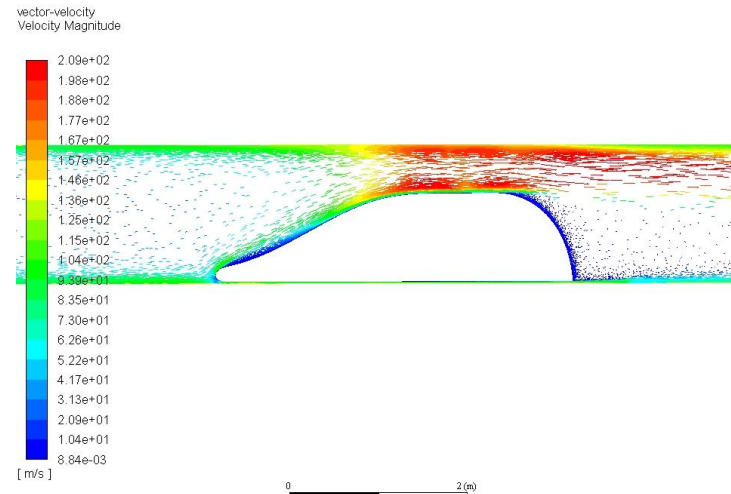
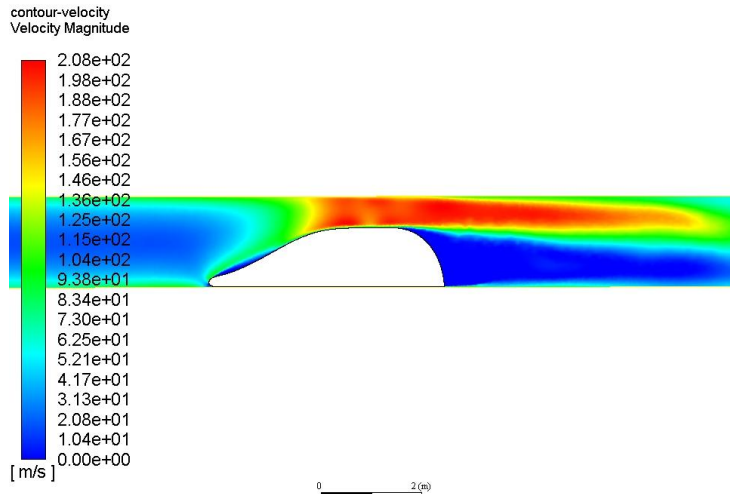
Drag: 109 N
Max air velocity: 443 m/s (Supersonic Flow)
Max Turbulent Kinetic Energy: 5719 m²/s²

Fuselage - 2D CFD Mesh

From the results of the previous iteration, namely the tail-up iteration, we ended up creating essentially a less-exaggerated flipped version of it, namely as depicted in the figure below. This “duck-billed” design ended up outperforming all the other designs we tested in 2D simulation environments, which is why we ended up testing it more extensively in the following four slides, namely for various velocity fields rather than just a single 120 m/s trial.

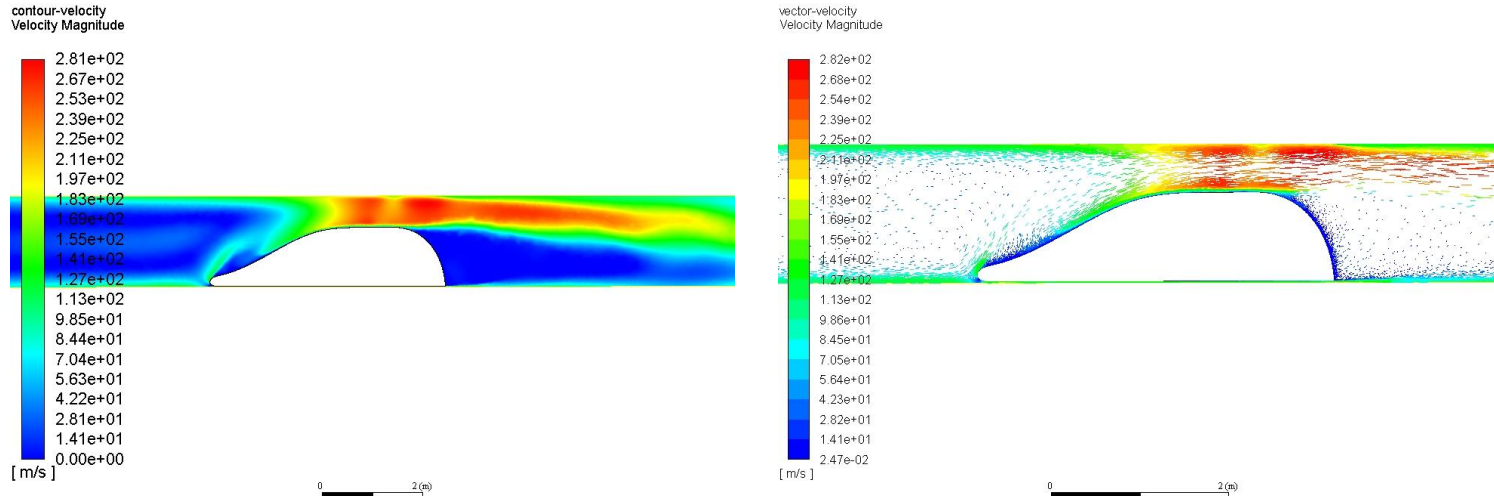


Fuselage - 2D CFD Results: 120 m/s

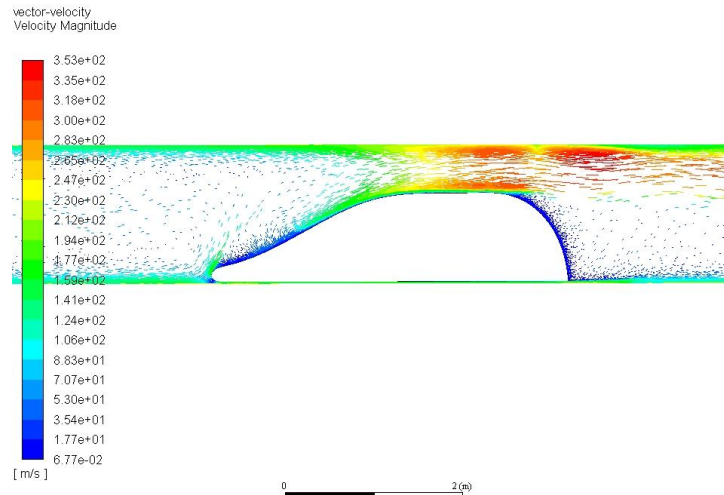
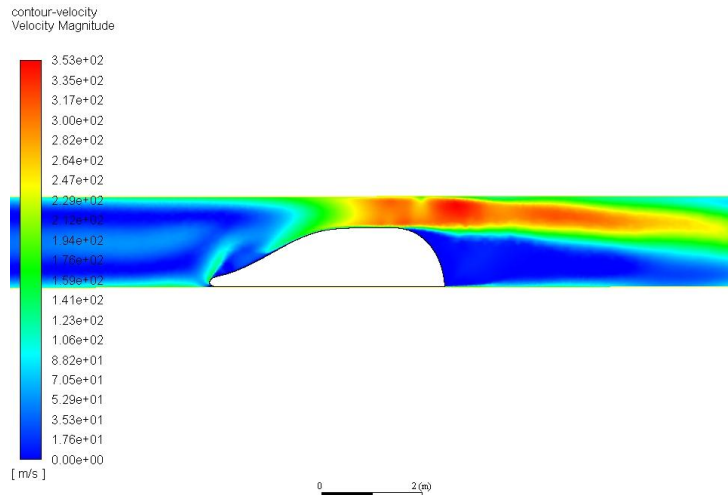


Drag: 20 N
Max Air Velocity: 208 m/s
Max Turbulent Kinetic Energy: 1483 m²/s²

Fuselage - 2D CFD Results: 150 m/s

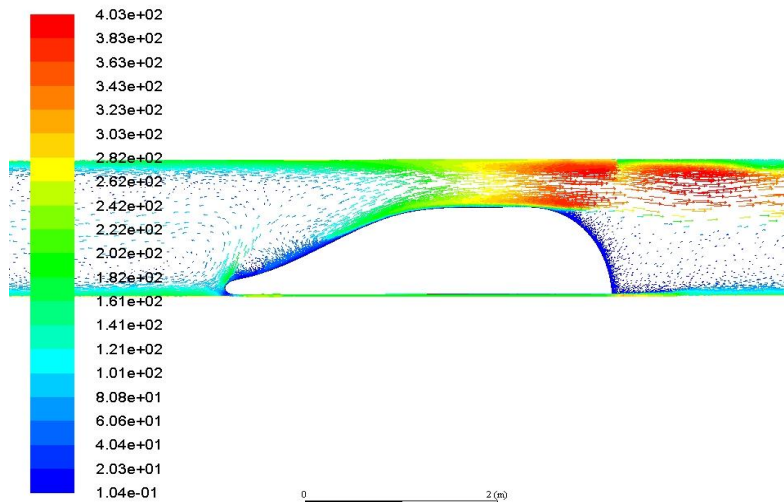
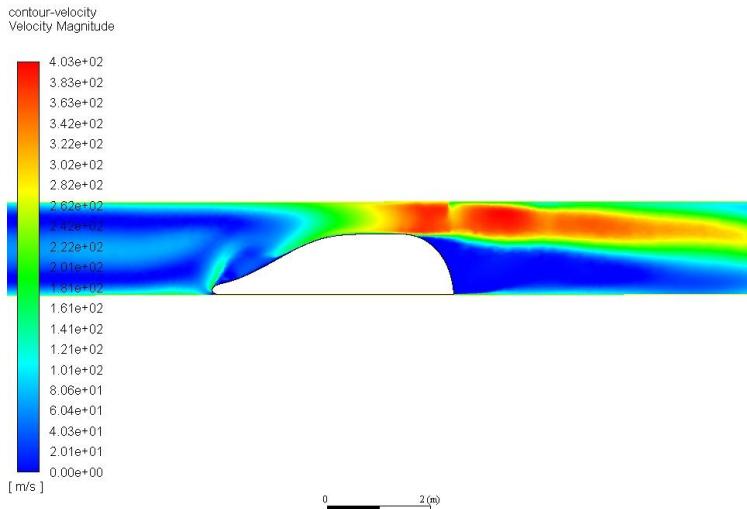


Fuselage - 2D CFD Results: 175 m/s



Drag: 48 N
Max Air Velocity: 353 m/s (transonic)
Max Turbulent Kinetic Energy: $2864 \text{ m}^2/\text{s}^2$

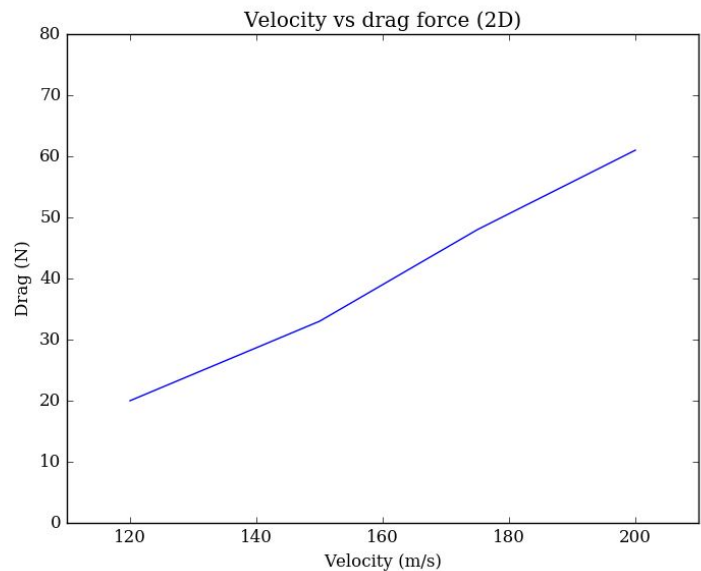
Fuselage - 2D CFD Results: 200 m/s



Drag: 61 N
Max Air Velocity: 403 m/s (Supersonic)
Visible shockwaves and flow separation
Max Turbulent Kinetic Energy: 3891 m²/s²

Fuselage - 2D CFD Discussion

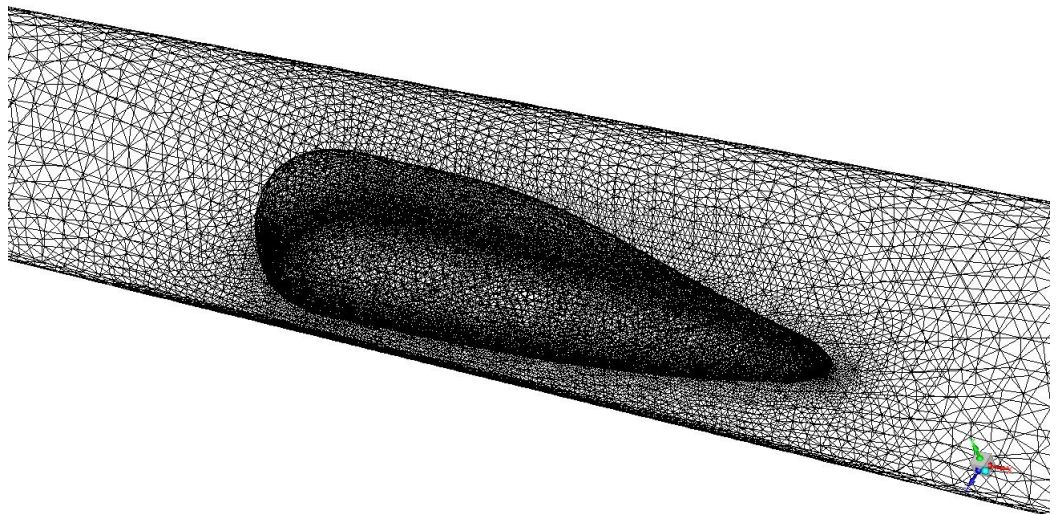
- We used 2D profiles to iteratively prototype our shell design, looking at key factors such as turbulence, max velocity, and force exerted on the pod
- Originally, our first design is based on a teardrop design, but it ended up having a pressure drag than the optimal design. Ultimately, the teardrop design is a good design aerodynamically for a subsonic *open air* system, but it is not optimal for hyperloop conditions.
- The next iteration was to alter the tail of the pod, and we show that a design that has the tip of the tail up would produce a supersonic flow at 120 m/s, which causes an increase in drag. This shows that the tail is already optimized in our initial design.
- We eventually settled on the “duck bill”, or “bullet train” design, which produced the least drag in our 2D simulations.
- The duck bill design allows for much higher speeds without inducing supersonic flow, at speeds in excess of 150 m/s



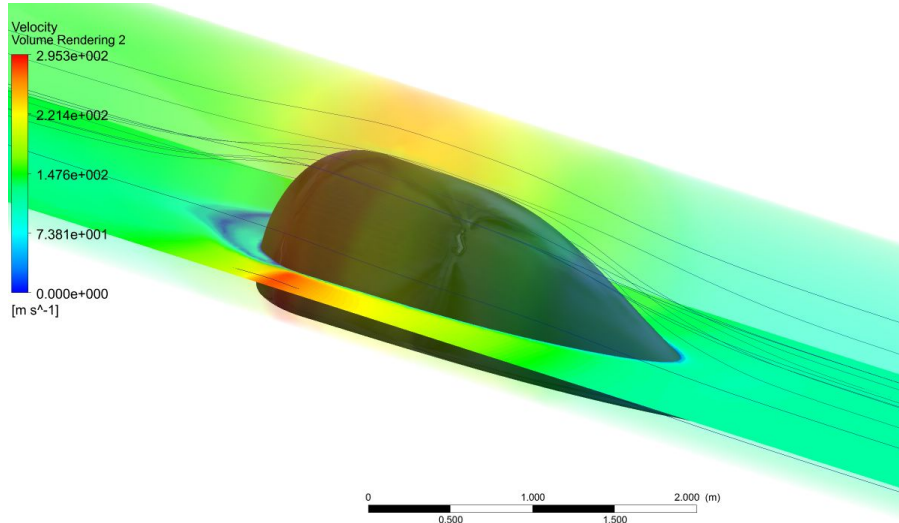
Fuselage - 3D CFD Setup

Parameters of CFD simulation, including:

- Freestream pressure: 100 Pa
- Size of the CFD mesh: **592,161** cells (final version)
- Size of the tube in CFD: 12x pod length (50m)
- Time stepping algorithm used in simulation: Density-based SST k-omega model
- Boundary conditions used for simulation:
 - Pressure far-field for the tube inlet and outlet
 - Symmetry BC used for the wall, and wall BC used for the pod itself



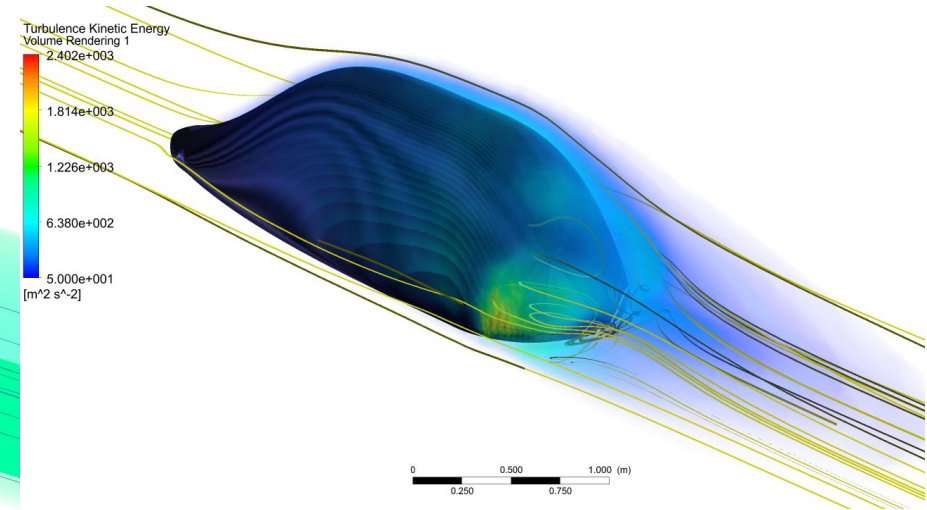
Fuselage - 3D CFD Results (at 120 m/s)



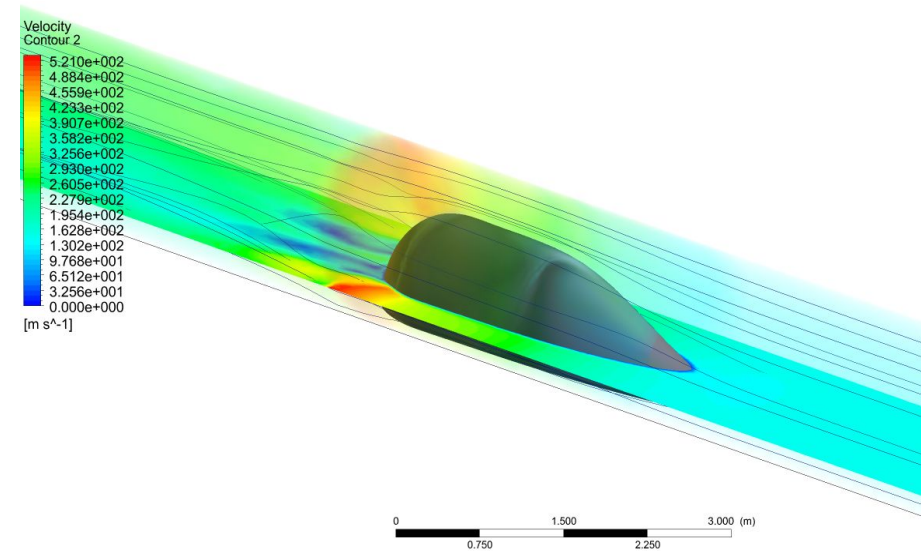
Max air speed: 295 m/s

Max Turbulent Kinetic Energy: 2460 m^2/s^2

Total Drag: 10 N

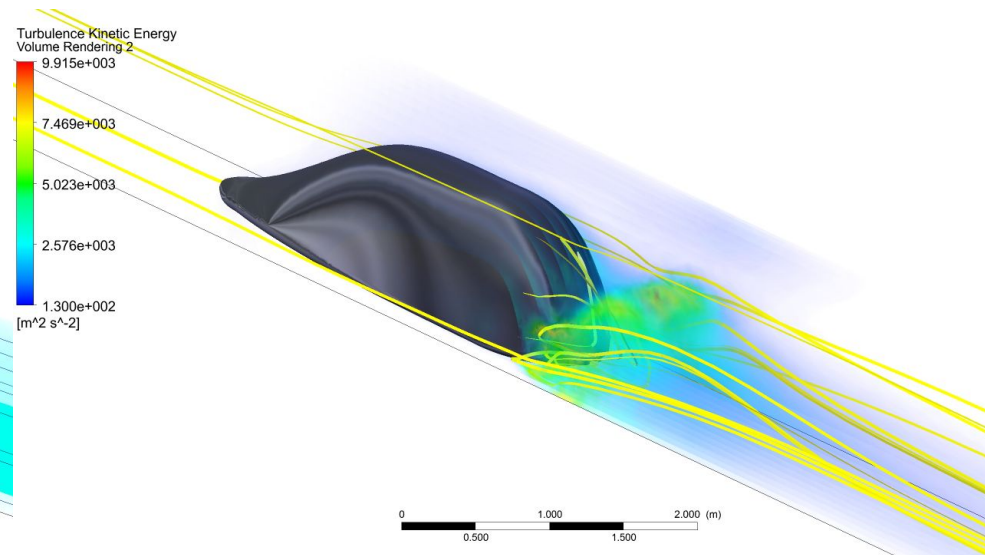


Fuselage - 3D CFD Results (at 200 m/s)



Max air speed: 521 m/s (supersonic flow)

Total Drag: 55 N

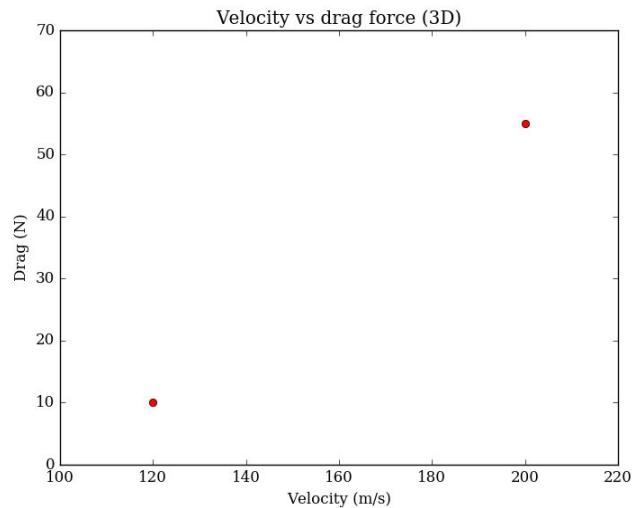


Max Turbulent Kinetic Energy: 9915 m²/s²

Fuselage - 3D CFD Discussion

From running the 3D CFD on our design, we evidently gleaned much more accurate estimates on numerical values and what we can anticipate in the final run. In particular, we observed:

- Drag force was lower than that of the 2D simulation
- We calculate a drag coefficient at the 120m/s range of $C_d = (2F_D)/(qv^2A) = 0.82$.
- The fluid flow is in the subsonic regime at 120 m/s, and becomes supersonic at 200m/s. Thus, the maximum
- Essentially the main obstacle of decreasing aerodynamic drag for the Hyperloop is overcoming the buildup of pressure in a closed tube system. Thus, the choices we made for our CFD setup, such as using a density-based solver for compressible flow, is the correct way to analyze aerodynamic drag.
- By optimizing our design in a restricted airflow environment where the diameter of the pod is near the diameter of the tube, we arrive at a shell geometry that is different from the conventional shape for an open-air system.
- Our analysis has the added benefit of creating a design that allows for a larger cargo capacity while having a smaller diameter pipe, reducing the construction and operating costs of creating and potentially increasing revenue.



Fuselage - Trajectory

To determine the overall maximum achievable velocity, we incorporated magnetic drag, air drag ($C_d=0.8$), and the inertial properties of the pod.

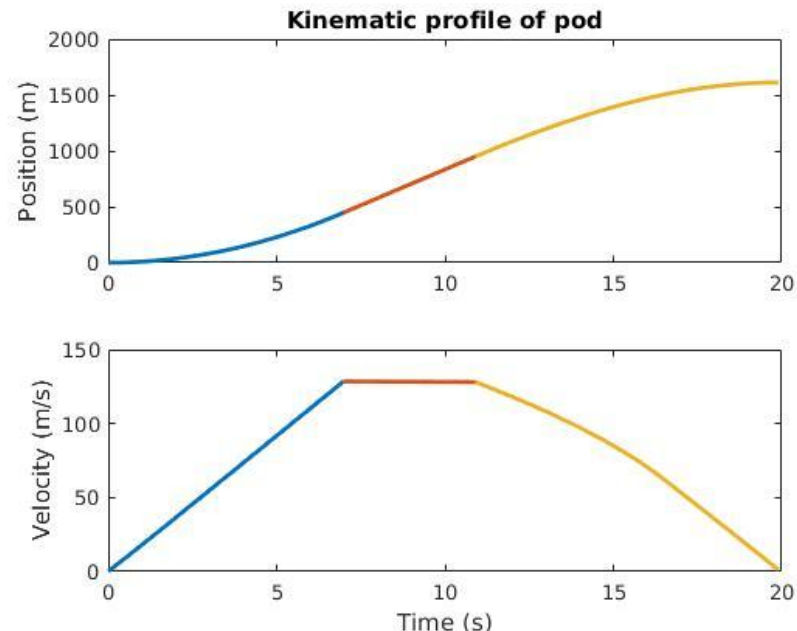
We will use the SpaceX pusher to achieve an acceleration of **1.9 g** from 0-450m.

The pod will cruise from 450-950m, only experiencing minimal aerodynamic drag and magnetic drag from the lift magnets.

The eddy current brakes deploy 650m before the end of the track, reaching a peak deceleration of **1.8 g**.

Thus, given the constraints of the test track, through numerical simulation, we found that the pod is capable of achieving:

- Top speed of **128.5 m/s**, or **287.4 mph**, by the end of the acceleration profile
- Stopping Distance (normal operation) of **650 m**
- Minimum test run time of **20s**.

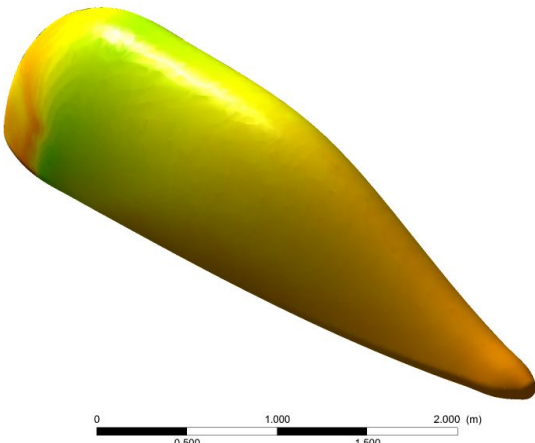


Fuselage - Heating Profile

Temperature
heat
[K]

3.142e+002
3.107e+002
3.073e+002
3.038e+002
3.004e+002
2.970e+002
2.935e+002
2.901e+002
2.866e+002
2.832e+002
2.798e+002
2.763e+002
2.729e+002
2.694e+002
2.660e+002
2.625e+002
2.591e+002
2.557e+002
2.522e+002

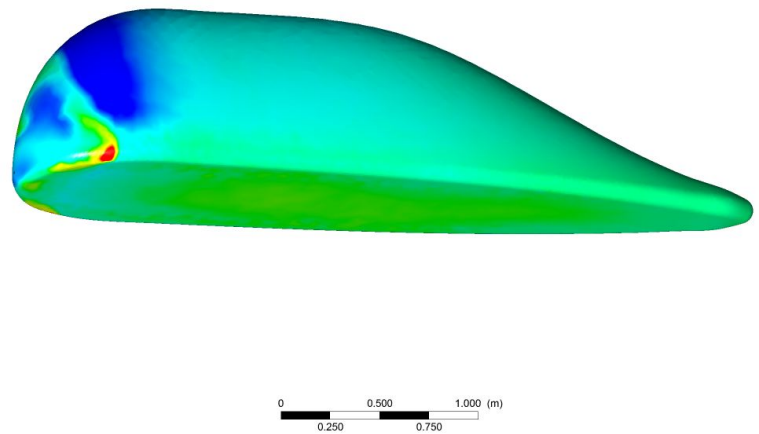
120 m/s



Temperature
Contour 3
[K]

3.696e+002
3.658e+002
3.619e+002
3.581e+002
3.542e+002
3.503e+002
3.464e+002
3.426e+002
3.387e+002
3.348e+002
3.310e+002
3.271e+002
3.232e+002
3.193e+002
3.155e+002
3.116e+002
3.077e+002
3.039e+002
3.000e+002

200 m/s



By performing a heating profile analysis on the shell profile, once again using Ansys CFD, we found:

- At 120 m/s, and at ambient temperature of 300K (27.9 C) and the CFD analysis reports a maximum increase of +16K at some locations on the shell (up to 43 C).
- At 200 m/s the maximum increase in temperature is +109K at a hot spot near the rear, raising the local temperature to 136 C.
- Since this is well within the operating range of the pod material (carbon fiber), there is very little reason for concern.

Fuselage - Predicted Vibration Environment

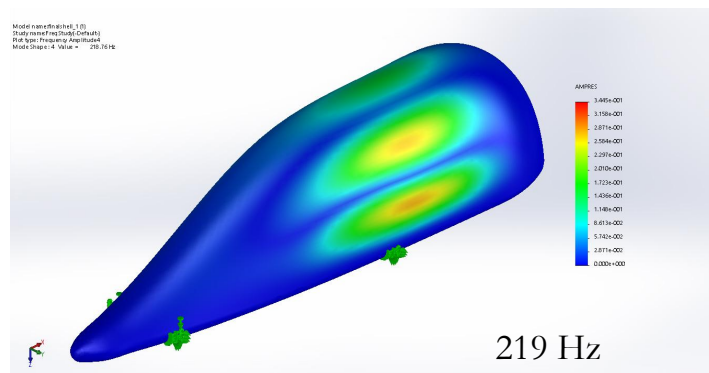
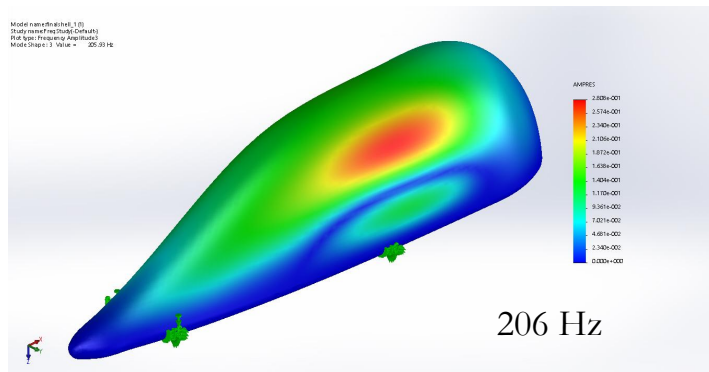
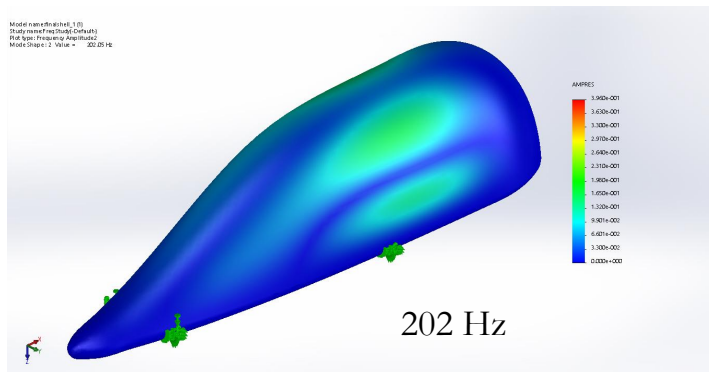
The fuselage was tested in five different frequencies to predict its vibrational response during travel: responses that could be produced by supersonic flow or vortices. We aimed to assure that the natural frequency of the carbon fiber was sufficiently different than the one encountered with air particles at high velocities. The five frequencies tested were:

1. 199.47 Hz
2. 202.05 Hz
3. 205.93 Hz
4. 218.76 Hz
5. 283.76 Hz

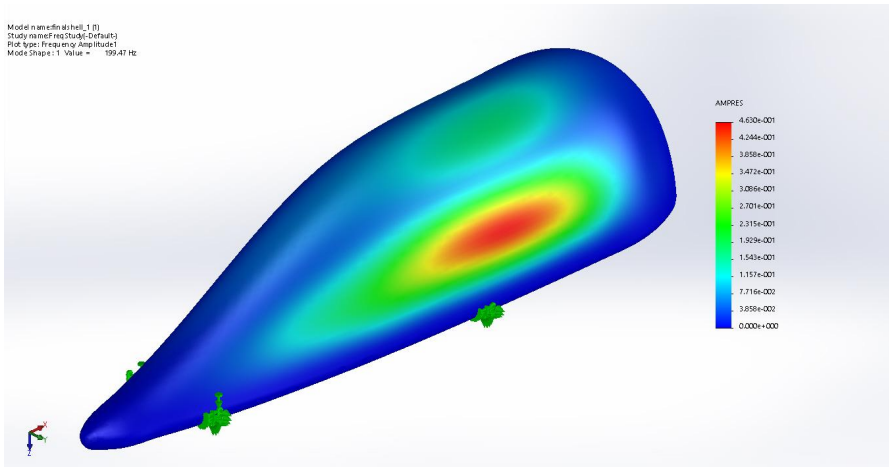
Results:

- The amplitude of response remains under 0.5 in every simulation, presenting that there is no significant deformation. The largest response was seen in the 199.47 Hz region, mainly affecting the sides of the fuselage. This could mean that the carbon fiber material is more susceptible to lower frequencies - something that we do not have to worry about in this context.
- The following steps in testing, to confirm our results, would be testing a small scale model in a wind tunnel. This could also include sampling a wider range of frequencies through sound.

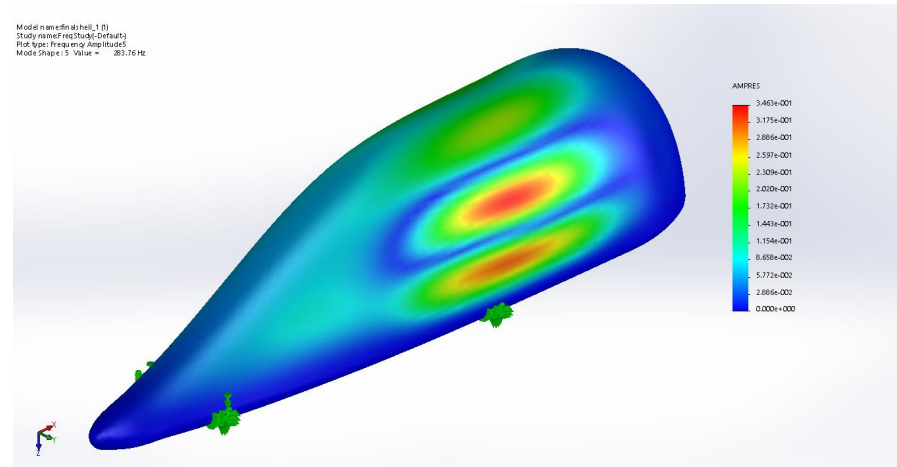
Fuselage - Predicted Vibration Environment (cont.)



Fuselage - Predicted Vibration Environment (cont.)

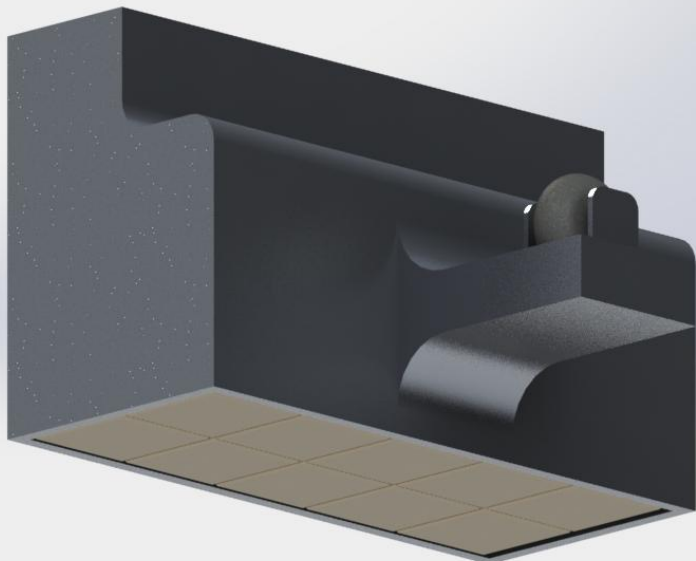


199 Hz



283 Hz

MAGNETIC SUSPENSION



Suspension - System Overview

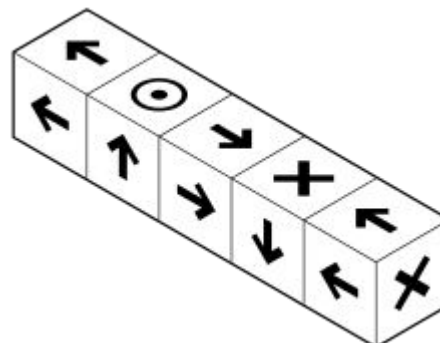
The direct purposes of the suspension are:

- Producing sufficient force to lift up the entire pod.

Similar to how it was presented in the PDR, the suspensions system consists of sets of Halbach array setups. Since the Halbach arrays only produce lift force when there is relative motion between the ground and the magnet system and only exceeds the corresponding drag force for sufficiently high speeds, there will be a wheel system on which the pod will roll prior to achieving significant enough speed to achieve lift via the magnet system.

The Halbach arrays have the following properties:

- Each consists of the standard five magnets magnets (right)
- The wavelength of the Halbach array λ is taken to be 5 times the length of a single magnet (2" x 2" x 2"), which we take to be 2 in, namely $\lambda = 10$ in.
- The magnets used will be neodymium, which we expect to exhibit B-fields of nearly .5 T



<https://upload.wikimedia.org/wikipedia/commons/thumb/c/c4/Halbach2.svg/250px-Halbach2.svg.png>

Suspension - Lifting Magnet Specifications

With cost minimization being a primary concern, we calculated the following to determine the ideal number and shape of the magnets, assuming:

- The surface of the aluminum track is uniform and fully conductive. The model applied for calculating lift/drag both assume an ideal conductor for the calculation, which we justified with a liberal safety factor of 2.
- We take the mass of the pod M to be 300 kg, and assume we are using 40 magnets for lifting (five magnets per Halbach array, two arrays per corner, one lift set per corner). The following equation calculates the total array area needed for these parameters.

Thus, solving the equations given in the original Halbach/Inductrack paper, we use the formulas provided for determining height:

$$A = \frac{Mg\mu_0 e^{4\pi y/\lambda}}{B_0^2} \quad \frac{\lambda}{4\pi} \ln\left(\frac{AB_0^2}{Mg\mu_0}\right) = y$$

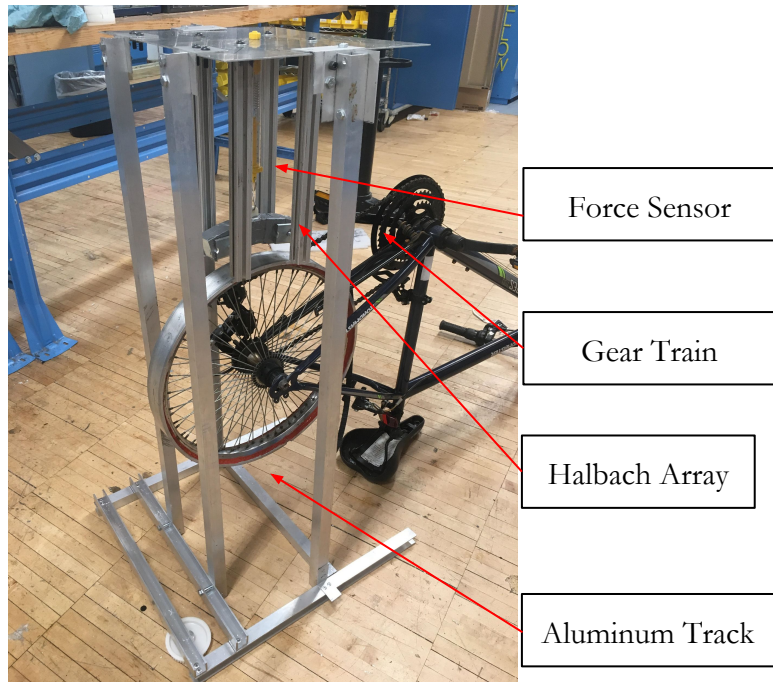
$$\frac{0.254m}{4\pi} \ln\left(\frac{40 * (0.0508m)^2 (.5T)^2}{(300kg)(9.8m/s^2)(4\pi \cdot 10^{-7})}\right) = y = 0.039m$$

Clearly, therefore, we are able to achieve the desired lift of 1.5 cm, with an additional 2.5 cm ($\sim 1''$) of suspension. We, however, can easily account for this in the springs that connect the chassis to the wheels, described in Slide 40.

Suspension - Lifting Magnet Test Apparatus

To model the lift the Halbach arrays will be able to achieve, we created a model lifting test apparatus. This similarly captures the relative speed we expect to achieve on the final pod run, where we chose instead to use **1" x 1" x 1"** magnets due to constraints on the physical test size. In particular, to capture the relative linear motion (i.e. ~ 140 m/s), we planned to rotate the wheel at $(140 \text{ m/s})/.5 \text{ m} = 280 \text{ 1/s}$, meaning we would need approximately 2000 RPM for the rotational speed of the wheel to create an accurate test. We created this through a gear setup, as pictured to the right, specifically:

- Halbach array only consists of a single array of half-scale neodymium magnets. That is, it only houses a single five-magnet set of Nd magnets, but produced the expected theoretical behavior (i.e. strong magnetic field on one side, nonexistent on the other)
- The Halbach array was attached to a force meter that determines how much lift we are experiencing.



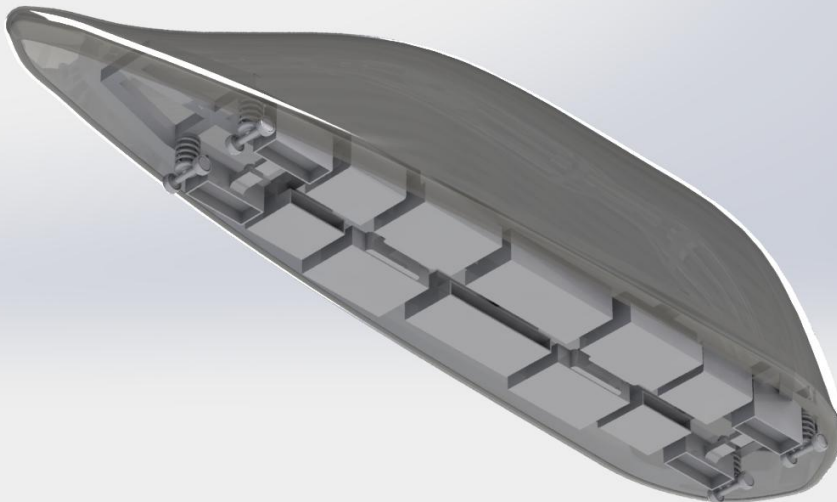
Suspension - Lifting Magnet Test Results

Due to failures in the motor setup, our wheel was not able to get up to the desired rpms. The large, first gear of the bike was powered by hand, which was connected to a smaller gear attached to the aluminum track. A surface track velocity of ~ 15 m/s was achieved. A weight was then placed on the Halbach array so that the force spring showed an initial displacement. Upon rotating the wheel up to speed, the Halbach array would levitate, thus compressing the spring; this indicated that lift had been produced to counteract the body force. We observed that as more weight was added, the Halbach array became harder and harder to lift because we were unable to get the wheel up to a high enough speed to produce enough upward force. At distance of 0.5 in away from the track, approximately 80 N of lift was generated at 15 m/s.



While we were unable to obtain solid data we gained a very qualitative experience and learned that even with slow speeds and small magnets, the Halbach array setup was able to generate a fair amount of lift as well as drag force. However, one major observation we took away from our tests was that the lift force seemed to overcome the drag forces once higher track velocities were achieved. At low speeds, the drag force was considerably strong. Additional testing is required to validate these claims.

BRAKING SYSTEMS



Braking - System Overview

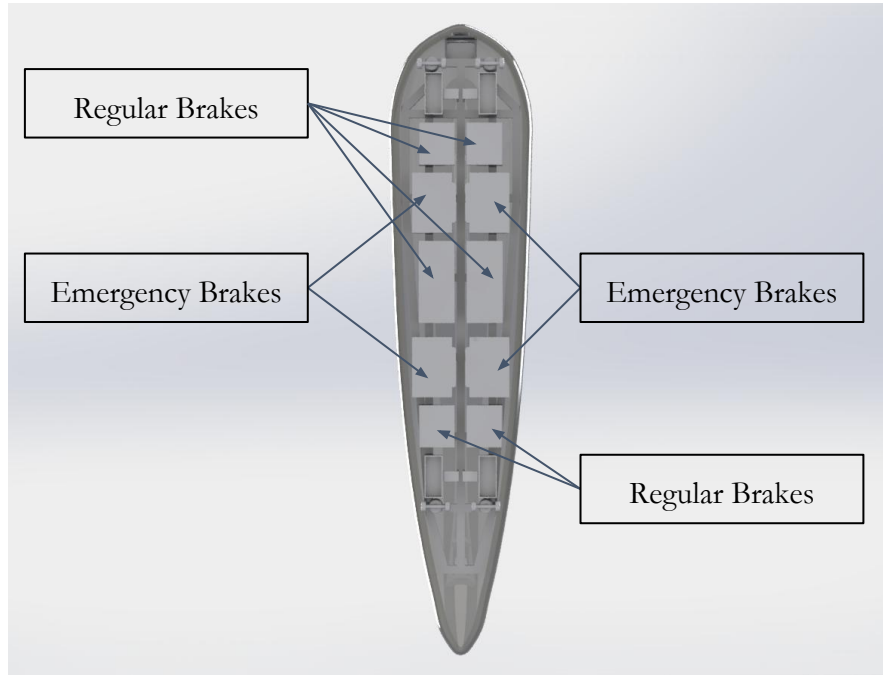
To avoid complicating the multitude of systems involved in the Fluxor pod, this system will use the same Halbach array set up as was used in the lifting arrays. In particular, we will have the same properties (B-field strength, wavelength) for the Halbach arrays. The braking system is split up as follows:

- **Actively-Controlled magnetic regular brakes:** Six sets of Halbach arrays mounted parallel to the T-beam that are extended out actively by linear actuators to be brought sufficiently close to the T-beam and produce magnetic drag.
- **Fail-safe frictional emergency brakes:** Four sets of springs held in place by power-activated locks such that power loss intentional or otherwise deploys the brakes.

Each brake system is independently capable of stopping the brake from the expected max speed of 130 m/s to a stop in 10 seconds. These brakes would be deployed in the following scenarios (more thoroughly expanded upon and presented in “Controls” section):

- **Regular:** Scenarios in which the regular brakes would be deployed
 - **Braking distance point detected:** Reach the point in the tube where should stop
 - **Off-nominal behavior detected:** Detect odd behaviors, i.e. overheating or sensor failures
 - **Off-nominal trajectory of pod calculated:** Determine that the pod is expected to crash/go off-course
- **Emergency:** Scenarios in which the emergency brakes would be deployed
 - **Off-nominal braking detected:** Detect being near the end of the tube but still moving too fast to stop in time
 - **Complete pod power loss:** Lose controls, which unlocks the pin locks and deploys emergency brakes

Braking - System Overview

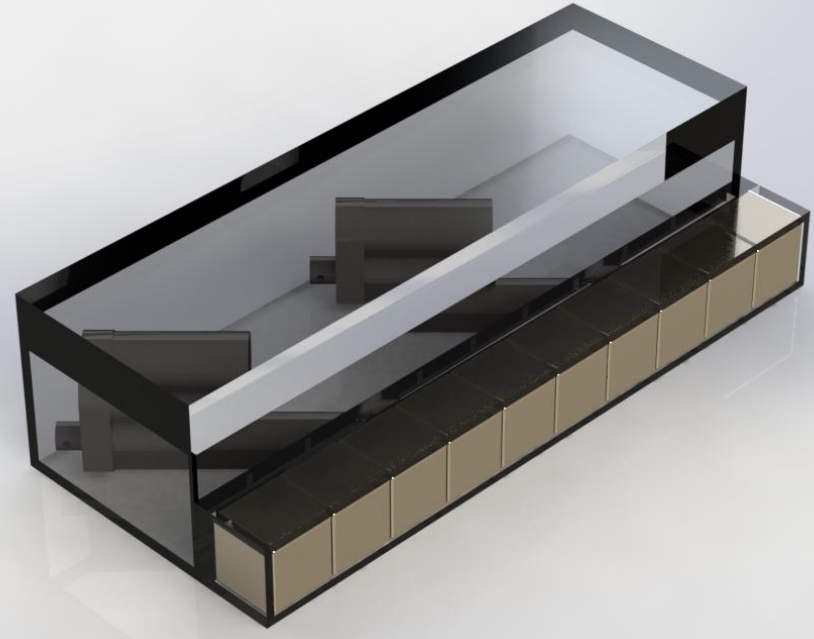


Braking - Regular Brakes

The braking system is deployed by linear actuators. Namely, there is one brake in each corner of the chassis along with two in the middle section of the chassis, which are twice the size of the corner brakes. The setup for these brakes are:

- **Corner brakes:** Single Halbach array, parallel to the T-beam with a single linear actuator
- **Extended middle brakes:** Two side-by-side Halbach arrays (i.e. a single, extended array) with a two linear actuators

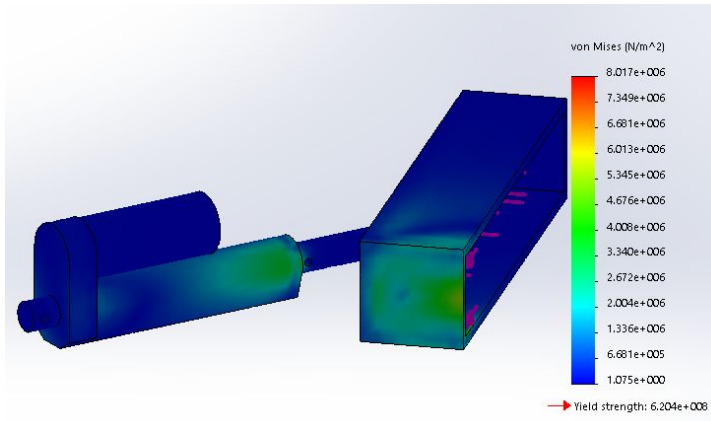
These brakes (explained fully in Controls section) are actively controlled through a single system, which will deploy all eight Halbach arrays to be .5 cm away from the center of the T-beam, inducing a strong magnetic drag force (and thus magnetic braking)



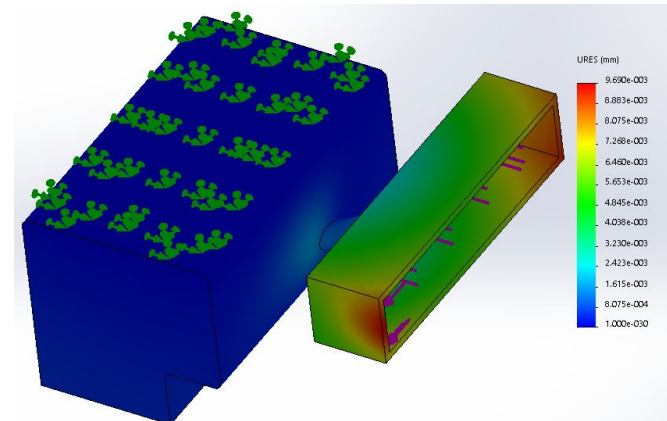
Braking - Regular Brake FEA

This simulation was to see that, when we extend the linear actuators to fully push the magnet housings, there is not too large of a load that either the housing or actuator shaft are experiencing as a result of the magnetic drag. From this simulation we see:

- The stress on the extender beam is largely insignificant, only reaching about 10 N/m^2 , meaning there is sufficient structural integrity to hold the brake together even when subjected to the magnetic drag force when close to the T-beam.
- The deflection caused by this force will not be asymmetric or result in a torque, thus allowing the magnets to remain in position to continue braking while close to the T-beam (implies continuous braking is a reasonable possibility)



Stress (N/m^2)

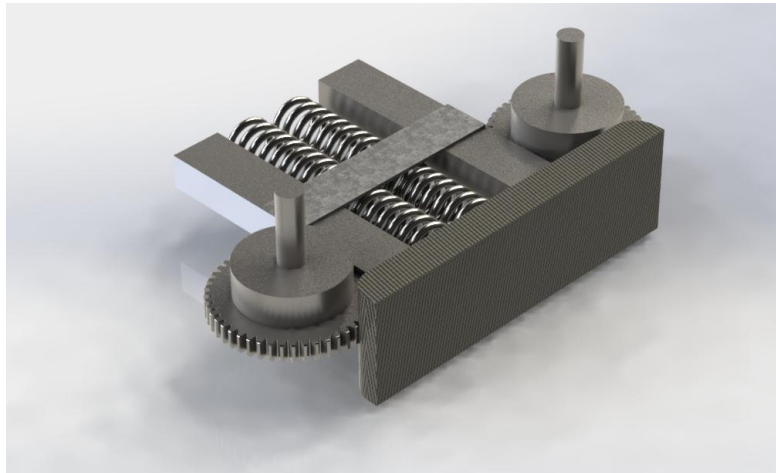


Displacement (mm)

Braking - Emergency Brakes Overview

The emergency brakes are, unlike all the other systems of the pod, a purely mechanically driven system. Four such emergency brakes are mounted on the chassis. At its core, the emergency brake consists of several braking pads being deployed to frictionally brake along the center of the T-beam. These brake pads are connected to springs, which are compressed against the housing wall, which are locked by powered ball-pin locks. When the ball-pin locks lose power, they will be retracted and cause the braking pad to be deployed and hit the T-beam.

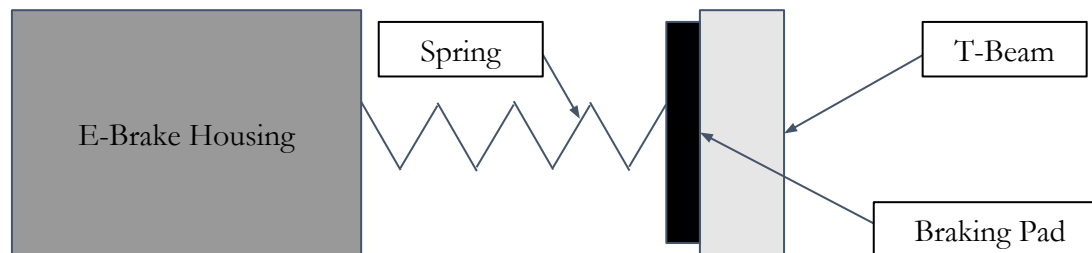
Each of the 4 springs exerts a force of ~ 500 N on the T-beam allowing for a total frictional braking force of ~ 2000 N. Each spring has a K-constant of 10,000 N/m.



Braking - Emergency Brakes Deployment

The emergency brakes, being fail-safe, are held in place by actively deployed ball-pin locks. If the power is cut, the pins will be removed from the sliding racks. This will allow the compressed spring to extend and push the brake pad into the T-beam. The spring will not be extended all the way but rather still be compressed behind its natural length to provide braking force against the T-beam. The brake pad is (LxWxH) 10" x 3" x 1" and will be made of Reinforced Carbon Carbon which excellent braking properties such as high temperature durability. Namely:

- The ball-pin locks will be actively controlled, such that when power is being supplied they are in lock position and retracted when not. Since this is a well-solved problem we do not concern ourselves with the internals of such a system.
- Two methods of deploying the brakes (described in the top-view extension in the figure below):
 - **Active deployment:** Stop the active supply of power through the controls system, which allows the springs extend out to their natural length and thus strike the brake pads onto the T-beam
 - **Passive deployment (fail-safe):** When power is lost or cut, the equivalent actions occurs as described above, since the two scenarios are equivalent after power is released from the pin locks



Braking - Emergency Brakes Heating

Below are the calculations to determine the heat load over time on the brake pads when braking on the T beam. It was assumed all frictional energy was converted to thermal energy, where we make the following assumptions:

1. $m_{\text{pod}} = 300 \text{ kg}$
2. $v_0 = 125 \text{ m/s}$
3. $v_f = 0 \text{ m/s}$
4. $\mu_k = 0.4$
5. (single brake normal force) $F_N = 1000N$
6. (thermal conductivity) $K = 40 \text{ W/(Km)}$
7. (mass density) $\rho = 2.45 \text{ g/cm}^3 = 2450 \text{ kg/m}^3$
8. (specific heat capacity) $c_p = kJ/(kg \text{ K})0.8 = 800J/(kg \text{ K})$

$$m_{\text{brake}} = \rho V_{\text{brake}} = (2450 \text{ kg/m}^3)(0.0762 \text{ m} \cdot 0.254 \text{ m} \cdot 0.0254 \text{ m}) = 1.20 \text{ kg}$$

$$K_i = \frac{1}{4} \cdot \frac{m_{\text{pod}} v^2}{2} = Q = m_{\text{brake}} c_p \Delta T$$

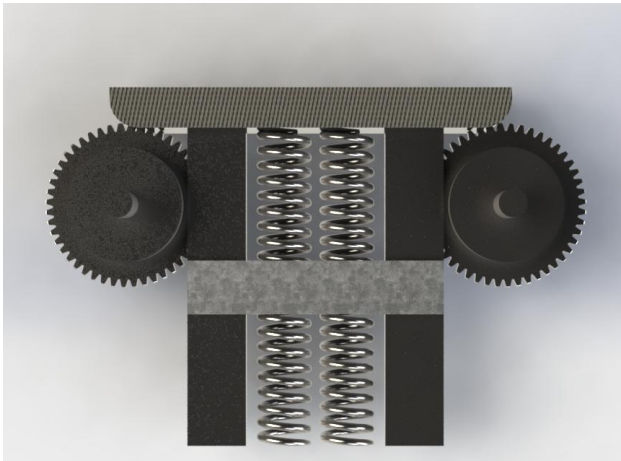
$$\Delta T = \frac{1}{4} \cdot \frac{m_{\text{pod}} v^2}{2m_{\text{brake}} c_p} = \frac{(300 \text{ kg})(125 \text{ m/s})^2}{8(800 \text{ J/(kg K)})(1.20 \text{ kg})} = 610 \text{ K}$$

From these calculations, we see that the braking heating is perfectly within reasonable limits, meaning we will operate within the melting point of the carbon ceramic material to be used for the emergency brake, as desired.

Braking - Emergency Brakes Retraction

After the E-brakes are deployed they are retracted using a motor and gear box system. The tripod extenders are lined with a rack, making it such that, after the E-brakes are deployed as discussed in the previous slide, they can be retracted using a motor/gear system. The motor is amplified by a 50:1 gearbox in order to rotate the gear attached to the rack slider. The rotating gear pulls the slider back into its casing against the force of the compressing spring. Once the slider is back in its non-fired position the pins are re-activated as described, returning the E-brake to its original state. In this case, we could use a motor of 3 Nm torque, since a gear ratio of 50:1 easily reaches the required:

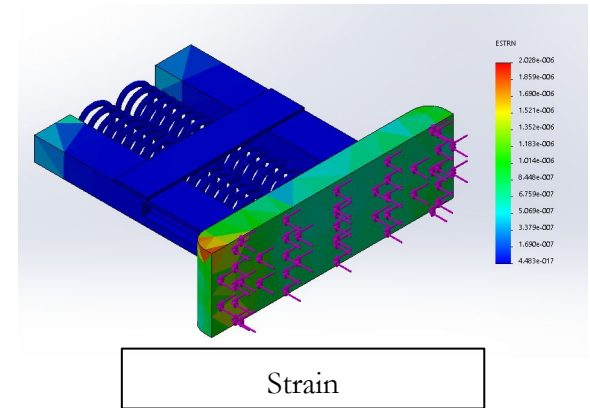
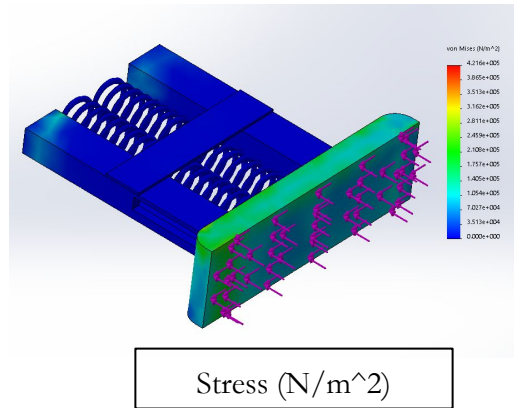
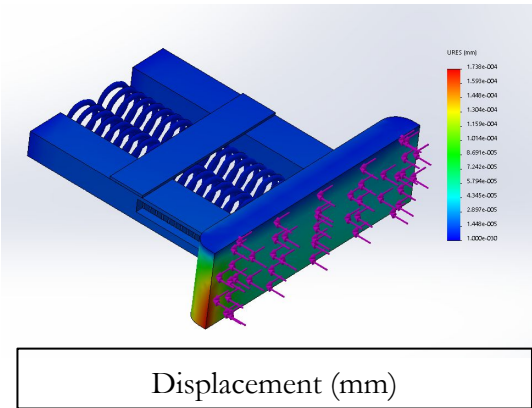
$$\tau = Fr = (500N)(.1m) = 50Nm$$



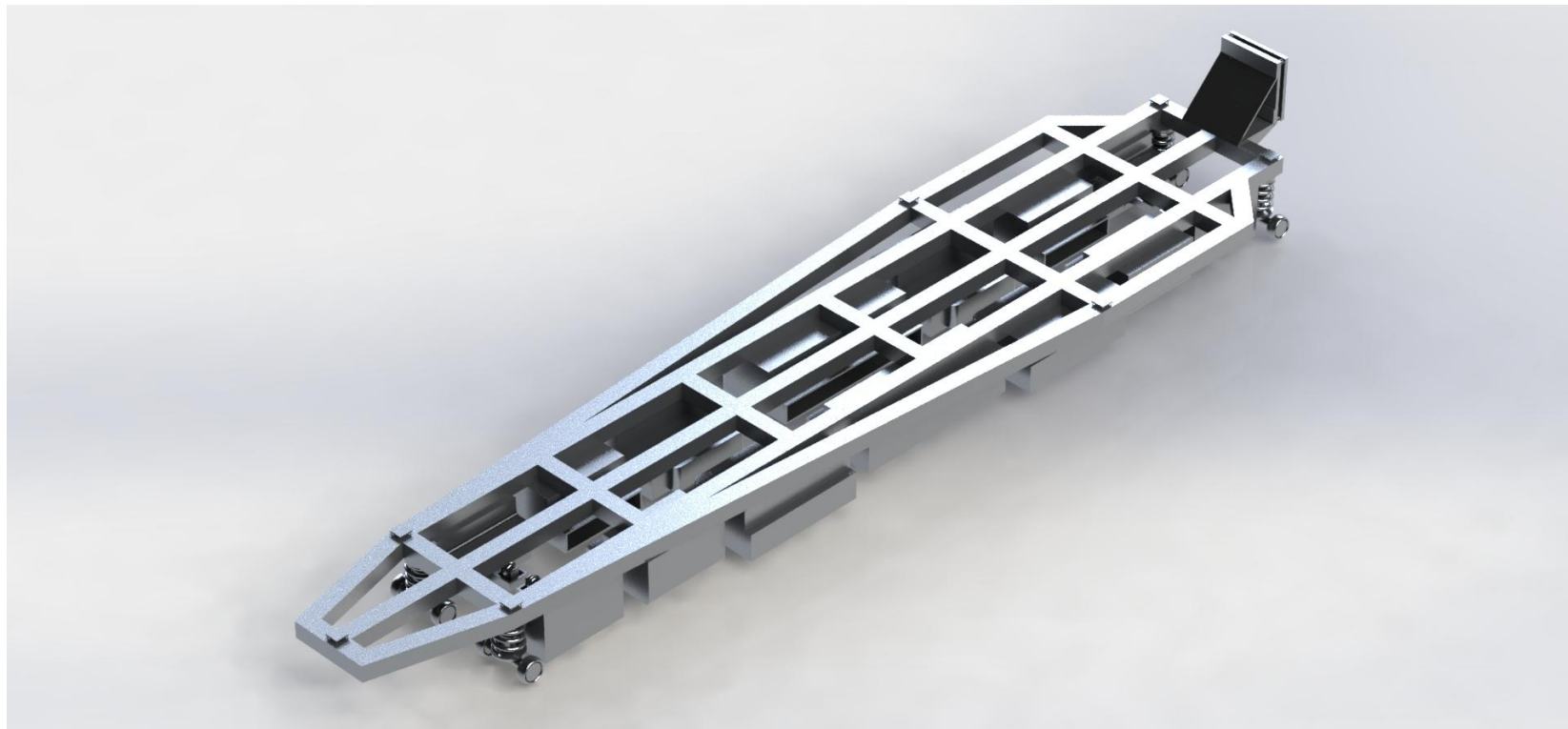
Braking - Emergency Brake FEA

This simulation was to see that (similar to the regular brake simulation), when we deploy the emergency-brake, there is not too large of a load that either the housing or extender beams shaft are experiencing as a result of torque from the frictional force between the braking pad and T-beam. From this simulation we see:

- There is negligible distortion of the braking-pad, namely it should not shear as a result of friction, which was expected of the braking material, otherwise there would be non-uniform braking across the pad
- The stress on the braking pad is sufficiently low (since pad has small area) that we expect its connection to the extender beam to remain intact



CHASSIS



Chassis - System Overview

The main purposes of the chassis system are to act as a vehicle through which:

- To house all the parts centrally in an organized fashion, namely the electronics, magnetic suspension, magnetic stabilization, power system, and wheels.
- Be sufficiently stable structurally as to hold the weight of the shell in addition to those components directly attached.
- Provide an interface to pick up acceleration from the pusher interface
- Provide a clean interface to connect to the shell of the pod

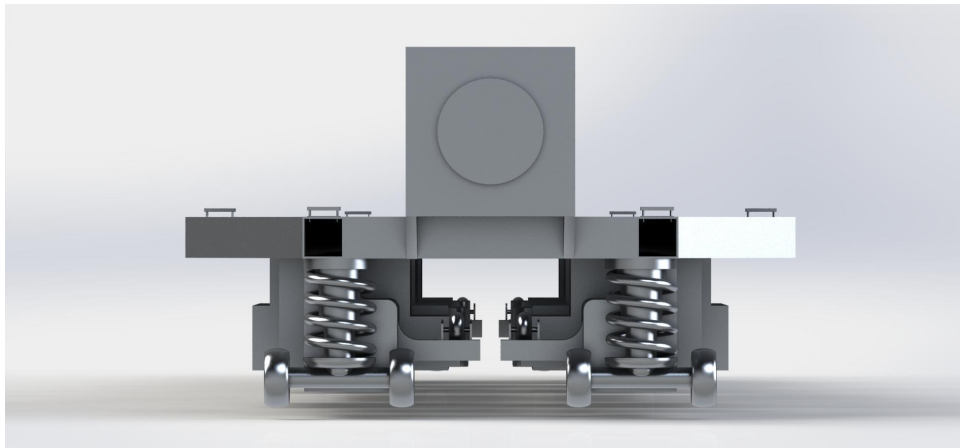
Applying these goals, our chassis has the following properties:

- Provides both a vertical and lateral stabilization mechanism:
 - **Lateral stabilizers:** also the magnets being used for regular braking, which will produce Eddy current repulsion if the pod gets unreasonably close to the beam.
 - **Vertical stabilizers:** The magnets used for lift will also naturally act as vertical stabilizers, since getting too close to the track will create a stronger force of repulsion, thus lifting the pod higher. If, on the other hand, the pod gets lifted too high, the magnetic interaction force will be much weaker, which will lower the pod. There, in addition, are physical rollers attached to the chassis, which will roll against the bottom of the top T-beam surface if lifted too high. This will cause the pod to mechanically slow down and, in turn, lower down as the magnetic force is proportional to the relative velocity.

Chassis - Wheel Overview

Since we need relative motion between the track and magnets to produce a force, we cannot directly initiate the magnetic suspension system. That is, we must have a method by which we can move before attaining sufficiently high speeds. In our case, we use regular wheels attached to springs such that, after attaining suspension, the springs are first decompressed fully and then the entire pod is lifted fully 1.5 cm. Namely, from before, we determined the magnets can theoretically achieve a lift of 3.9 cm, meaning we have an extract 2.4 cm over which we simply wish to decompress the four springs. Since the pod weighs $(300 \text{ kg})(9.8 \text{ m/s}^2)$:

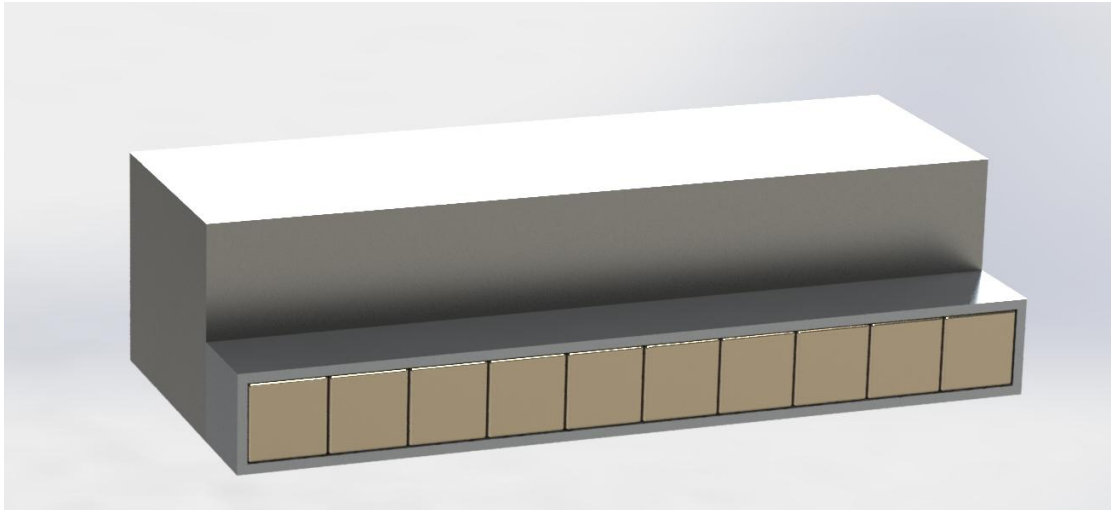
$$k = \frac{1}{4} (300 \text{ kg})(9.8 \text{ m/s}^2) / (.024 \text{ m}) = 30,625 \text{ N/m}$$



Chassis - Lateral Stabilizers

By doubling the braking magnets as lateral stabilizers, we gain significantly in cost and mass efficiency. Namely:

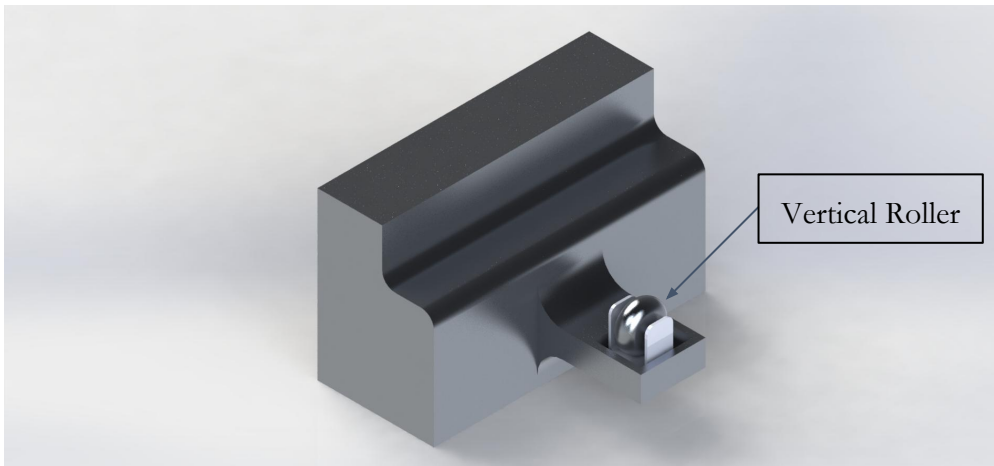
- **Lateral stabilizers:** Since the regular brakes are constantly facing the T-beam, i.e. are mounted perpendicular to the central portion of the T-beam, they will produce Eddy currents that similarly produce magnetic forces perpendicular to the beam. This causes repulsion, and thus, prevents the pod from getting too close/laterally crashing into the T-beam. Further, as the magnets are mounted on the chassis symmetrically about the T-beam, this keeps the pod centered in the tube



Chassis - Vertical Stabilizers

By doubling the lifting as a vertical stabilizer respectively, we gain significantly in cost and mass efficiency. Namely:

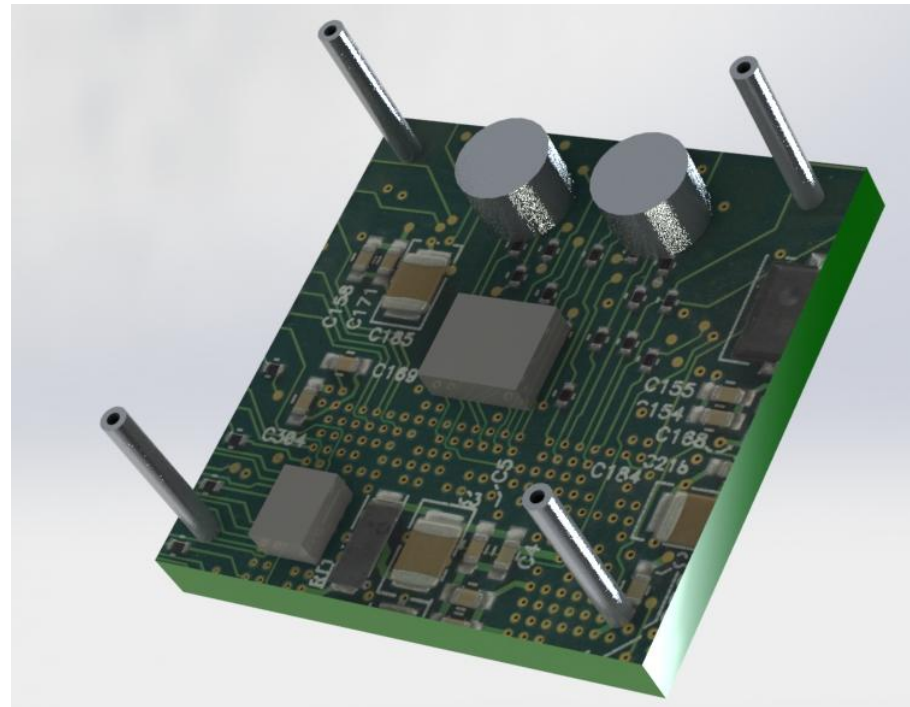
- **Vertical stabilizers:** In a nearly identical manner, the Eddy currents produced in the track will be directed upwards (i.e. away from the ground) and have magnitudes inversely proportional to how far away the pod is from the track, which keeps the pod in a relatively fixed location in the z-axis. Similarly, the additional rollers (pictured below) will roll against the T-beam, preventing any significant damage to either the track or pod and causing the pod to lower through friction braking.



Chassis - Removable Shell

Clearly, in the final pod, it is desirable to have a method by which the shell can be easily removed as to allow for easy maintenance and upgrades to the pod. In particular, we chose an electropermanent magnet (E.P. magnet) system, where an E.P. magnet is a system that becomes magnetized after being activated. It differs from standard electromagnets as a constant voltage is *not* required. Instead, after the first burst of energy, the system becomes permanently magnetized.

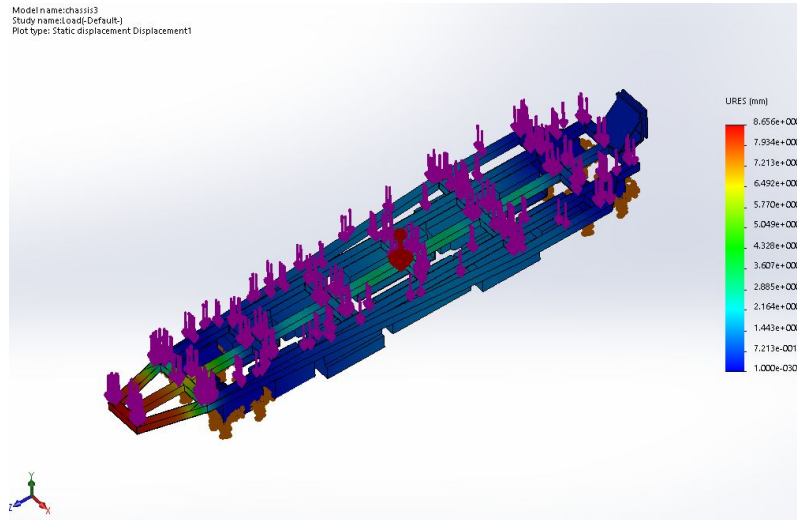
Thus, we use such E.P. magnets, in pairs, where we have corresponding locations on the chassis and shell where they are mounted, in opposite orientations. In doing so, when power is initially sent to both systems, they orient magnetically in opposite directions, causing them to attract. When power is sent again, both magnets demagnetize, thus allowing easy removal of the shell.



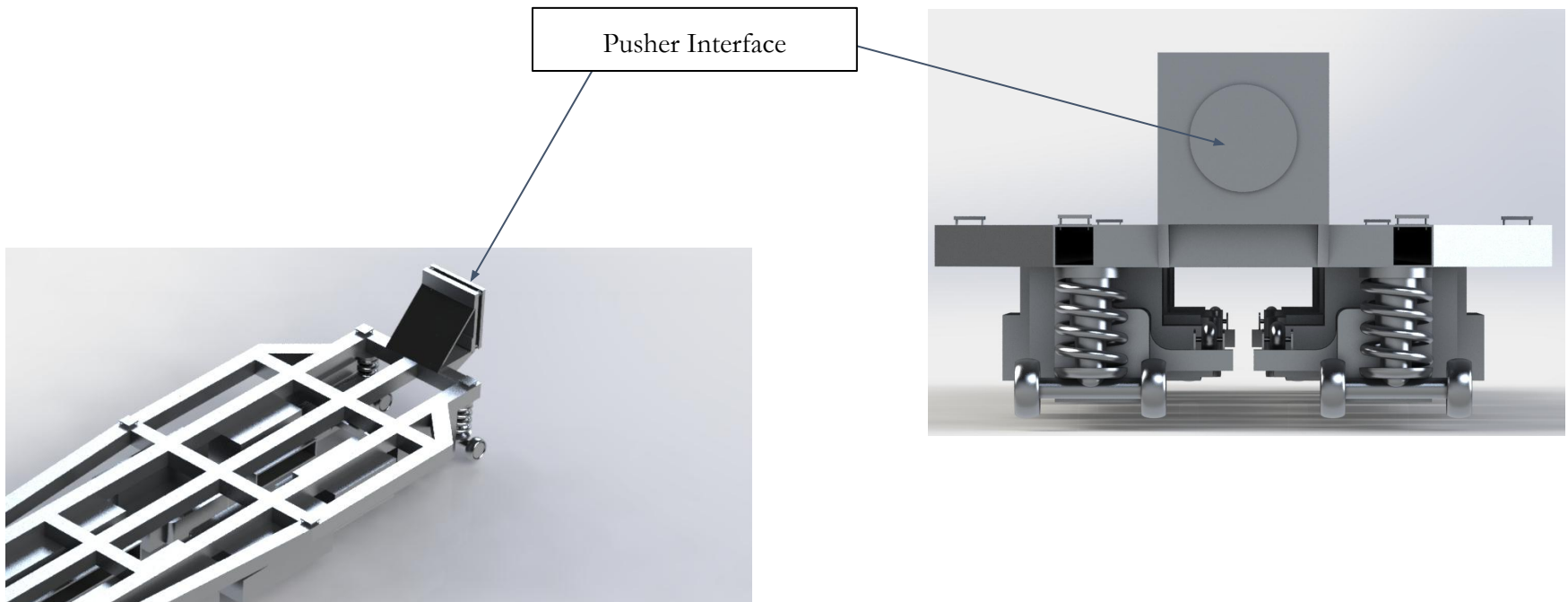
Chassis - Load Capacity FEA

From this simulation we saw:

- By applying a load onto the chassis body, where we expect to house all onboard passengers and other cargo, we found the max load capacity of the body was *very* conservatively 2000 kg. Specifically, 2000 kg (shown in figure below) was the point at which we first produced a deformation/displacement of **1mm**. It is quite possible we can easily accommodate 10,000 kg before considering the displacement too significant (i.e. .5 cm), meaning that our load capacity is approximately ten metric tons.



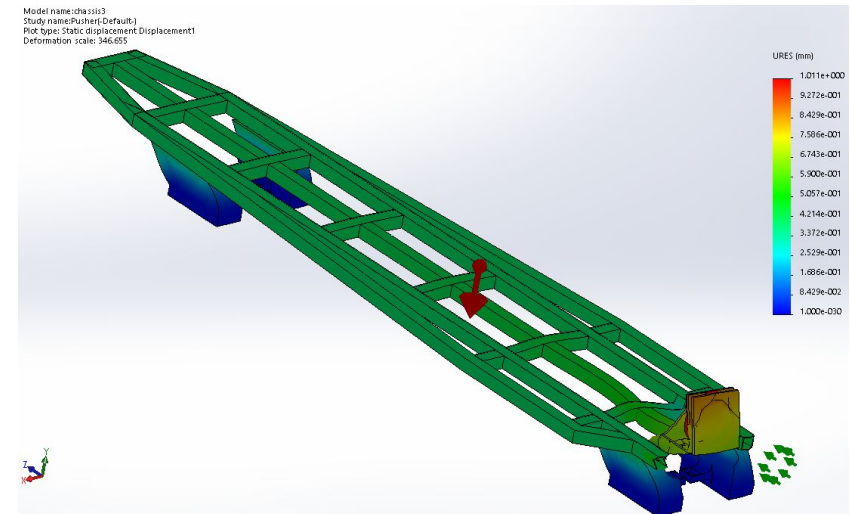
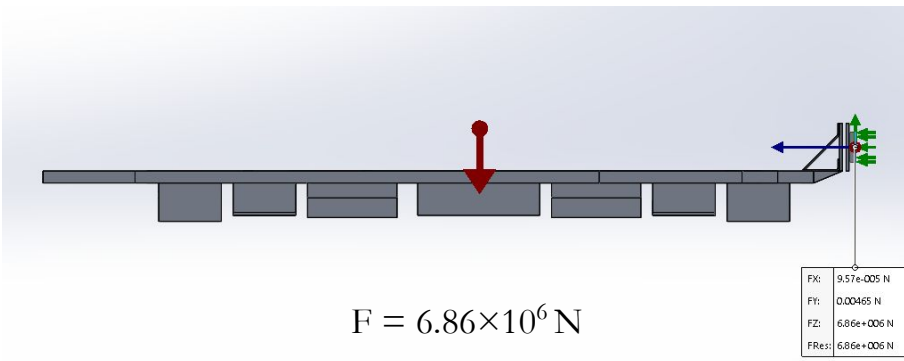
Chassis - Pusher Interfaces



Chassis - Pusher FEA

From this simulation we see that, even with a significant safety factor in the force being exerted by the pusher interface:

- The maximal deflection of the chassis is expected to be < 1 mm, meaning no significant distortion is expected. In turn, we expect the chassis is designed fully well for the purpose of being accelerated by the the pusher interface



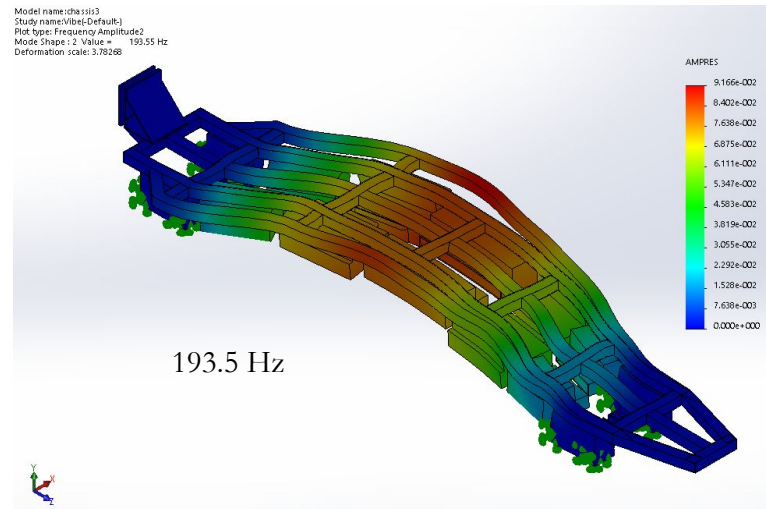
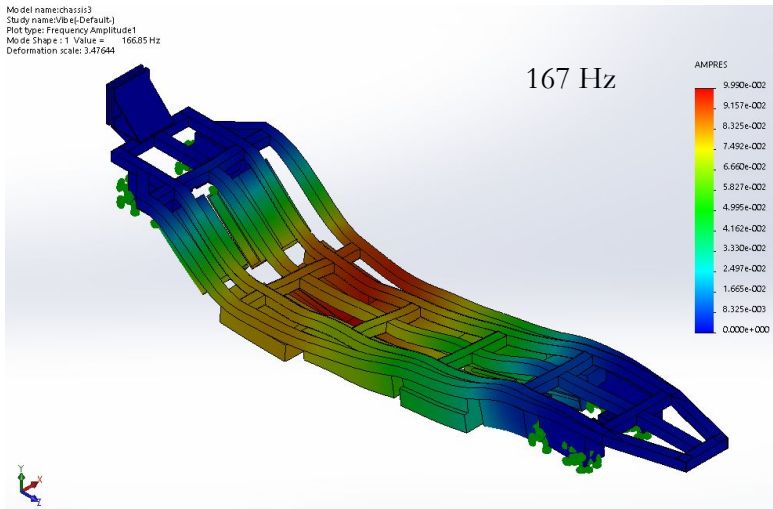
Chassis - Predicted Vibration Environment (cont.)

Similarly to the fuselage frequency analysis, we tested five frequencies on the chassis to predict undesired behavior in the tube. The graphs are deformed to a scale that visualizes the way the wave travels through the aluminium. Potential vibration in the chassis poses a much larger risk since essential components are at risk, such as the electrical system or suspension. Therefore it is crucial to understand the magnitude and frequency of vibration that the chassis might be susceptible to. The 5 frequencies tested were:

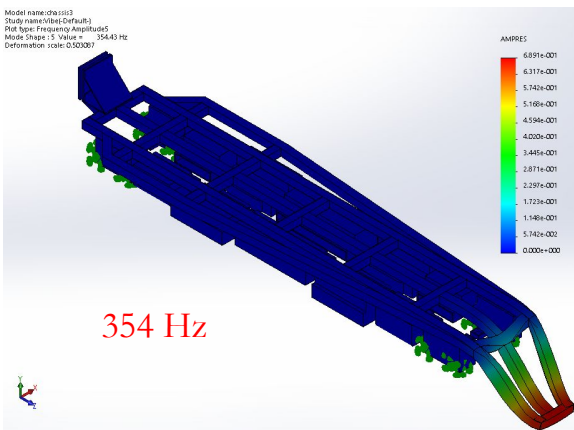
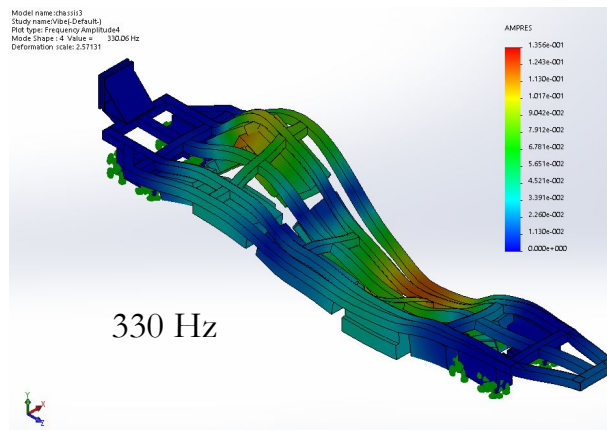
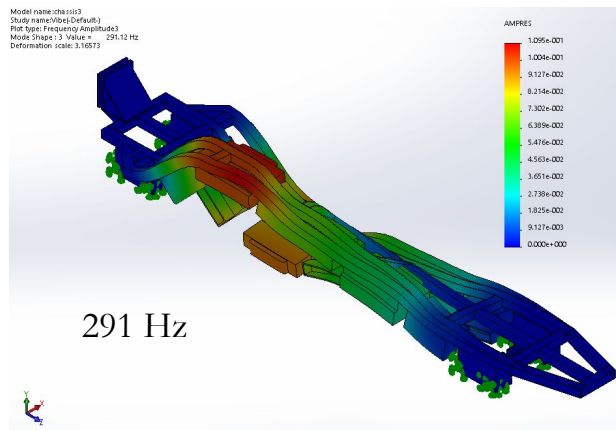
1. 166.85 Hz
2. 193.55 Hz
3. 291.12 Hz
4. 330.06 Hz
5. 354.43 Hz

In this case, we saw a larger response than the carbon fiber fuselage. Test 5 resulted in a amplitude of ~ 0.7 , in the front of the chassis. We must be aware of this situation of when placing instruments or cargo near this area, which could distort readings, damage components, or result in undesired behavior. For this reason we placed our electropermanent magnets in a triangular configuration facing the front of the pod. In case the front magnet disengages, the two others bordering the light blue section on graph 5 should retain the integrity of the shell without vibrational interference.

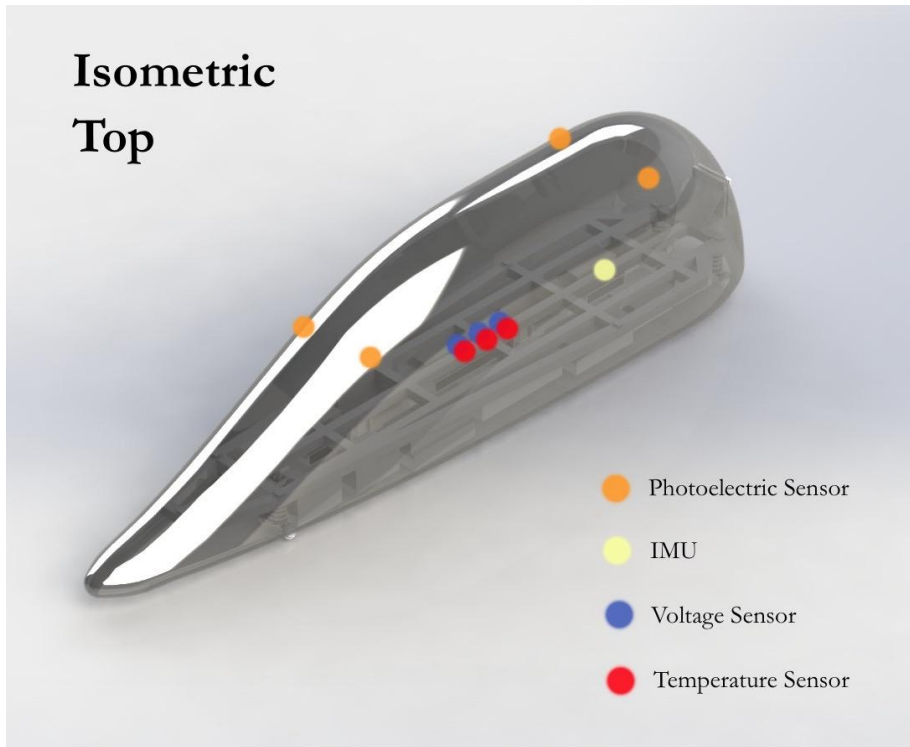
Chassis - Predicted Vibration Environment



Chassis - Predicted Vibration Environment (cont.)



CONTROLS



Controls - Software Overview

There are three primary purposes of the software, namely:

- **Monitoring:** To ensure the pod is operating as expected, we will monitor aspects of the pod operation (detailed in the following slides). This will primarily be used for testing purposes, i.e. would not be integrated in the final design of the HyperLoop pod. An example of this is a hall effect sensor to measure B-field strengths of the permanent neodymium magnets used for suspension.
- **Predictive:** By integrating the sensor readings into a Kalman filter, we will accurately determine the location of the pod in the tube, both with respect to the entire track and the cross section of the tube.
- **Corrective:** Integrating the predictive outputs, we would want to correct the pod trajectory and operation. Specifically, we will be actively controlling the deployment of the regular brakes (not necessary for the emergency braking).

The communication and processing of the sensors will all be handled with a centralized Raspberry Pi 3 controller, meaning there is no slave/master system incorporated in the design. In doing so, we reduce the number of independent systems required for operation, thus reducing the possibility of direct failure of the controls system.

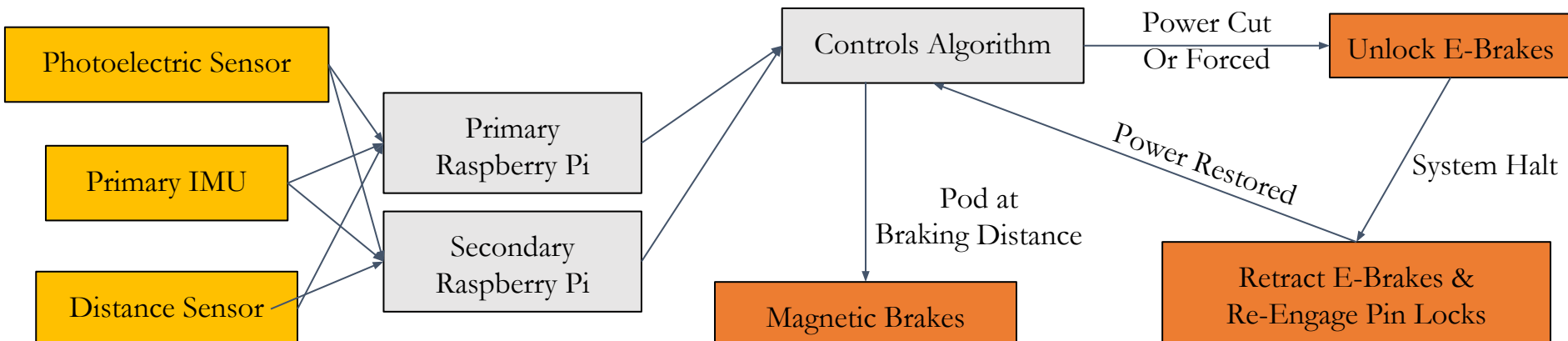
In line with such a redundancy system, we will have two Raspberry Pis hooked up, with one designated as the primary controller. In the case that gets corrupted or fails mid-run, power and control would be automatically transferred to the other RPi.

In adopting a Raspberry Pi 3 Model B, which has a quad-core 64-bit ARM Cortex A53 and operates at 1.2 GHz, we decided to primarily use Python for development, which can be easily sped by integrating in Cython. The GUI output will be developed either using Python or a web-framework, per our findings of which is more convenient.

Controls - Software Flow

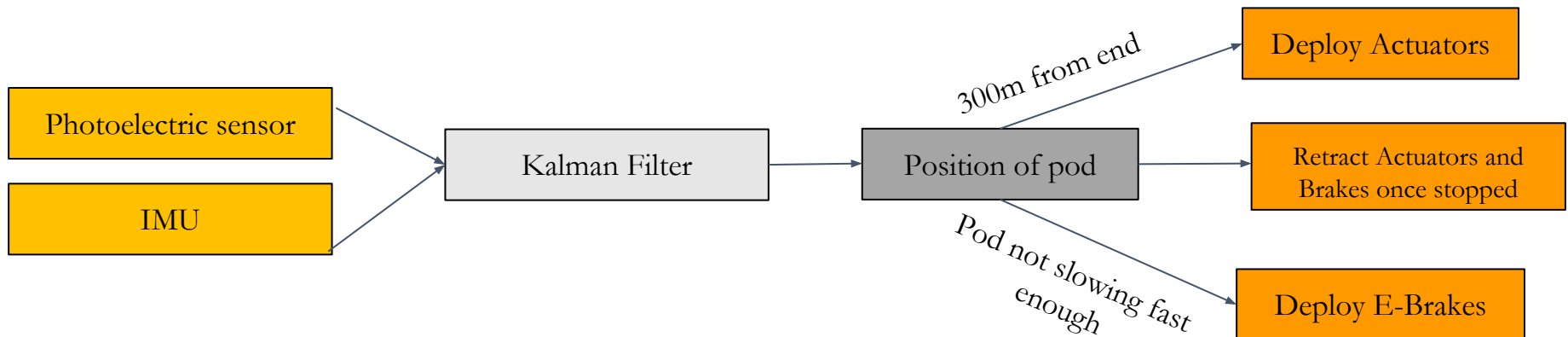
The following readings would be fed into the Raspberry Pi controller:

- The motion of the pod is monitored by the inertial mass unit (Model: KVH 1725), an integration of three gyros (Model: DSP-1750) and three MEM accelerometers, with six degrees of freedom
- The photoelectric sensors (Model: QMI9-0P-0A) monitor the reflective tapes along the top of the tube and lasers (distance sensors; Model: GP2Y0A41SK0F) keep track of the distance of the pod from the central rail and from the subtrack surface. These inputs will then be filtered into the Kalman filter.
- The controls algorithm will read the inputs and adjust the systems accordingly. Deploy e-brakes if there is a power cut detection or deploy regular magnetic brakes if pod is at brake distance.



Controls - Detailed Brake Controls

- Position data from the IMU will be corrected with photoelectric sensor data (which detects distance from the reflective tapes along the track) through a kalman filter, which will allow the pod to accurately determine how far it has traveled and how close it is to the end of the track
- When the pod is 300 meters from the end of the track, the raspberry pi will send a signal to deploy the actuators. If we detect that the pod is not slowing down enough, the e-brakes will be deployed. Once the pod has stopped, the actuators can be retracted and the motors will be activated to retract the e-brakes, if necessary.



Controls - Sensors Breakdown

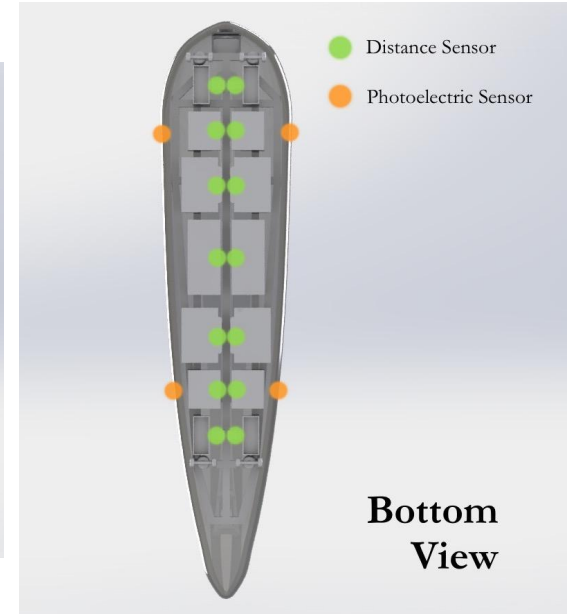
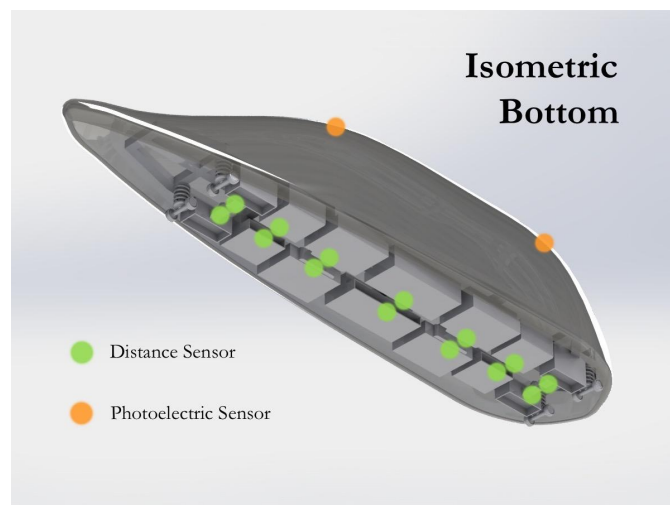
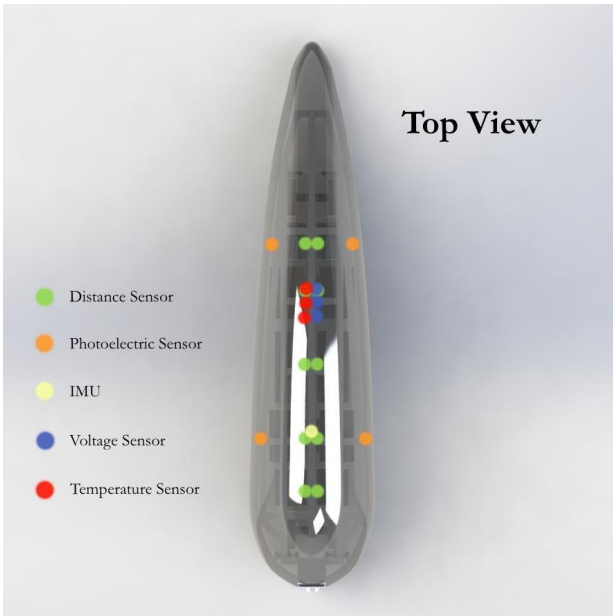
In line with the sensors' goals, this is the list of particular models and purposes for the sensors:

Sensor	Model	Number	Total Cost	Purpose
IR-LED Distance Sensor	GP2Y0A41SK0F	14	\$110.04	Measuring distance from central rail (4) and vertical levitation (4)
Photoelectric Sensor	XUB5BPANM12	4	\$156.00	Detection of the reflective tapes
IMU	KVH 1725	1	~\$1,200	IMU unit with three gyros and three accelerometers
Temperature Sensor	Si7050/1/3/4/5-A20	3	\$3.00	Monitor the temperature of the batteries
Voltage Sensor	1135_0 Phidgets	3	\$57.00	Ensure that batteries are giving out voltage

Final Sensor Costs	\$1,526.04
--------------------	------------

Controls - Sensors Placement

These particular sensors are distributed throughout the chassis and frame as shown below:



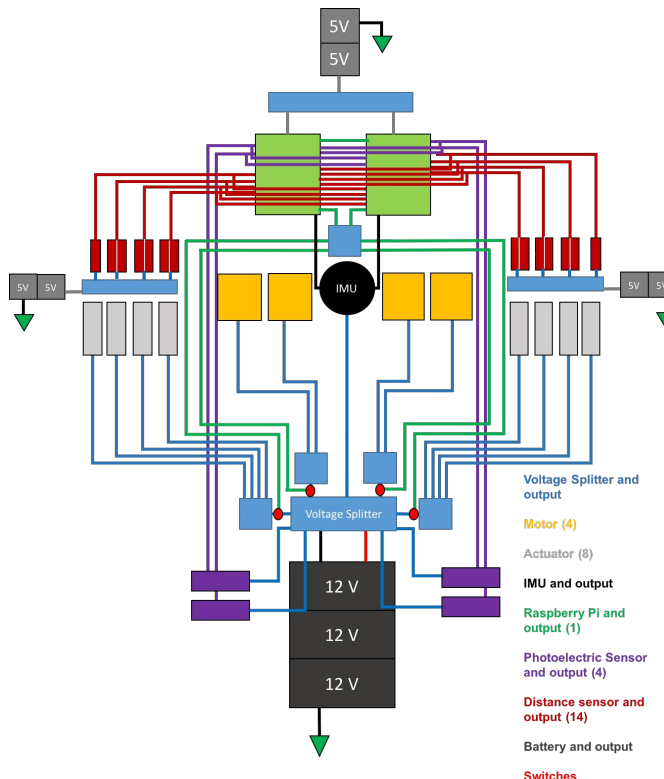
Controls - Power Requirements

These are the power requirements for sensors, motors, and actuators:

- Motors: ~12 volts
- Actuators: 12 volts
- IMU: ~12 volts
- Photoelectric sensors: 10 - 30 volts
- Distance sensors: 4.5 - 5.5 volts
- Voltage sensors: 5 volts
- Temperature sensors: 1.9 - 3.6 volts
- Raspberry pi: 5 volts

There will be 3- 12 volt batteries in parallel to power the IMU, motors, photoelectric sensors, and actuators. There will be 4 sets of 2- 5 volt batteries in parallel to power the other sensors and raspberry pis, which do not consume a substantial amount of energy. Temperature sensors and voltage sensors will be attached to the 12 volt battery supply to monitor its heating. They will have their own set of 2 parallel 5 volt batteries, and will relay data to both raspberry pis, just like the other sensors.

Controls - Wiring Schematic



Sensors will be powered primarily by 5 volt battery supplies, and distance, photoelectric, voltage, and temperature sensors will transmit data to both raspberry pis, which are connected and can both regulate the pod, should one fail. When the sensors detect that the pod is nearing the end of the track, the pis will send a signal to switches regulating power for the motors and actuators. The switches will close and current from the 12 volt power source will be allowed to flow to the motors or actuators to prepare for breaking. The pis can also choose to close the switches any time during the duration of the trip to correct for error such as tilting or to stop the pod prematurely depending on sensor data.

Controls - Transmission and Control Point

To ensure we are able to properly communicate from the egress station to the pod throughout the length of the track:

- Pods and control point will transmit data using TCP for reliable message delivery. Pod will transmit telemetry data while the control point will transmit remote commands such as engaging e-brakes
- The control point will run industry-grade programs, such as Grafana and InfluxDB.
- The controls dashboard is fully customizable for complex modeling and data visualization. Modules on Grafana will generate system heat maps and raw metric graphs. A button will be customized and added for the e-brake command



Example of a Customized Grafana Controls Dashboard
(Beekman: <https://www.cupfighter.net/uploads/2016/e.png>)

COMPETITION WEEKEND DETAILS



Testing - Vacuum Compatibility Analysis

Based on our on-board facilities, the considerations for compatibility with the vacuum was pretty direct. Namely, as most of our critical pod functionality from a mechanical standpoint relies on magnets, there is little concern with having degradation of performance in vacuum as compared typical test environments. In particular, as magnetism is inherent to the materials, these properties will remain constant despite changes in environment. As for other subsystems:

- Metallic corrosion will be negligible within the vacuum as the testing will only last for short periods of time.
- Our sensors do not require a medium to function since they are all gyroscopic, optic, or analog based (none are sonic based), and therefore are all compatible with the vacuum environment.
- Batteries are also rated for vacuum levels of pressure so even in the event that the shell is punctured they will function normally. We will use lithium ion batteries.

Testing - Safety Features

With safety as a primary concern in our design, we kept redundancy at the forefront. Specifically, as was highlighted in the respective sections, we have the following safety features:

- **For braking failure** (determined if the regular brakes are insufficient to stop in time or were not deployed correctly)
 - Sensors would actively detect that the pod has not slowed down sufficiently, namely that the predicted slower speed was not attained, which would cause the redundant emergency brakes to be actively deployed.
- **For suspension failure/inhibition during acceleration** (acceleration does not occur to desired extent)
 - In this case, the pod would simply ride on its wheels, as the wheels are not actively deployed. In other words, since the loss of contact between the wheels and track is fully contingent on achieving the suspension, the springs would never retract, which means the pod would continue to roll on the tracks until all the initial speed is dissipated through frictional interactions with the track or braking. While less than ideal, this does not damage the pod nor does it damage the track.
- **For catastrophic failure** (complete loss of power)
 - An emergency brake system that fails safe in the case of a total power loss that too can be controlled actively (if desired to be deployed when power present). This allows the system to not only be activated in the case of losing power but also if any monitored activity is significantly different than expected.
 - Back up batteries will be used to engage the motors and retract the E-brakes after coming to a complete stop. The pod will then continue down the track on its wheels as a means of exit.

Testing - Safety Features Cont.

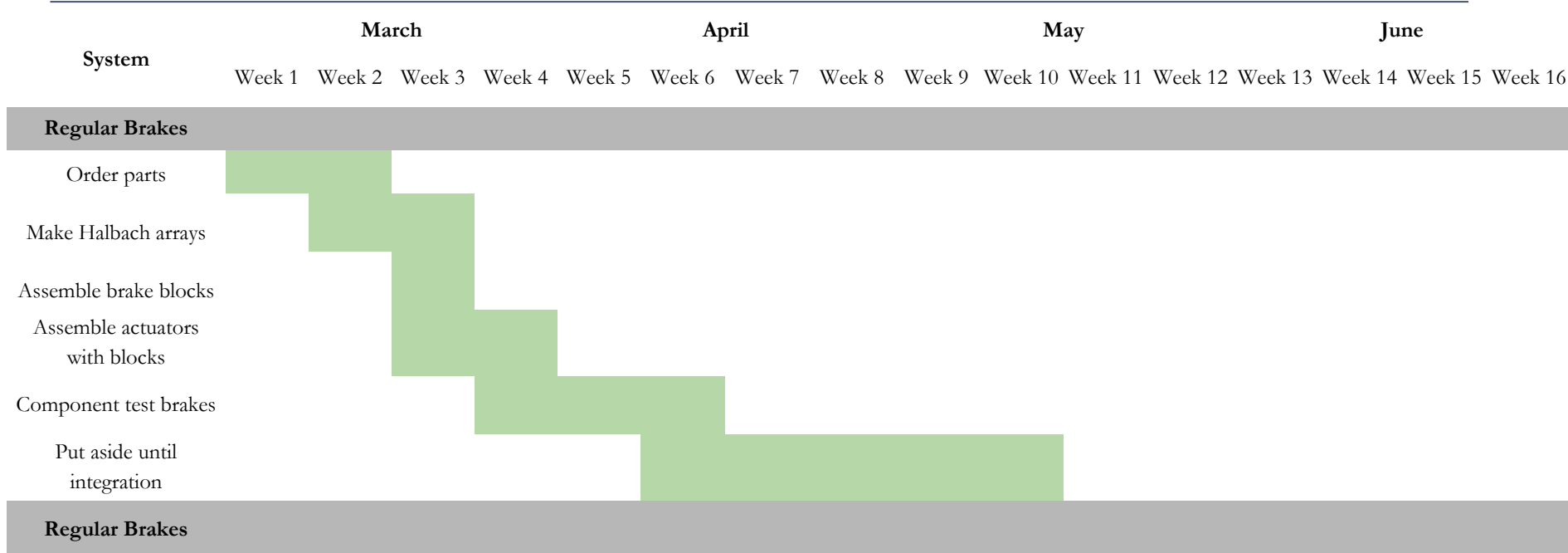
- **For tube/hull breach** (deformations in the tube create extreme pressure gradients)
 - The strength of our shell with its carbon fiber body would be able to maintain structural and corporeal integrity even under drastically changing pressure environments. This includes the case of rapid pressurization as result of a tube breach and even potential breaches of the shell itself.
- **Single point of failures:**
 - **Overheating batteries** (high temperatures detected by thermal sensors near the battery)
 - The pod, via the control algorithm, would switch to a redundant set of batteries that are not overheating. In the rare case that both sets of batteries are overheating then the E-brake would be activated and the pod would be forced to a complete stop to prevent any further damage.
 - **For controls failure** (corruption or loss of power to a microcontroller)
 - The redundant controls system (secondary RPi) assumes primary control upon sensing the primary Raspberry Pi is no longer sending confirmation signals, in turn monitoring the sensors and controlling end effectors.
- **Pod stop:** If so desired, the pod can be actively stopped with the execution of a STOP command, which deploys the regular brakes (i.e. deploys actuators) and, if insufficient braking is detected, also the emergency brakes.
- **Fault tolerances** (for levitation and braking)
 - Suspension: As described previously, any faults will largely be mitigated as a result of the stabilization systems
 - Regular Brake: If insufficient braking is achieved, the emergency brakes too can be actively deployed.
 - E-brake: If the emergency-brake achieves insufficient braking, it will instead gradually slow the pod. After a certain point, the pod will no longer be travelling sufficiently fast to levitate, which creates physical contact and, thus, additional frictional braking between the track and wheel.

Testing - Scalability (Full-Scale)

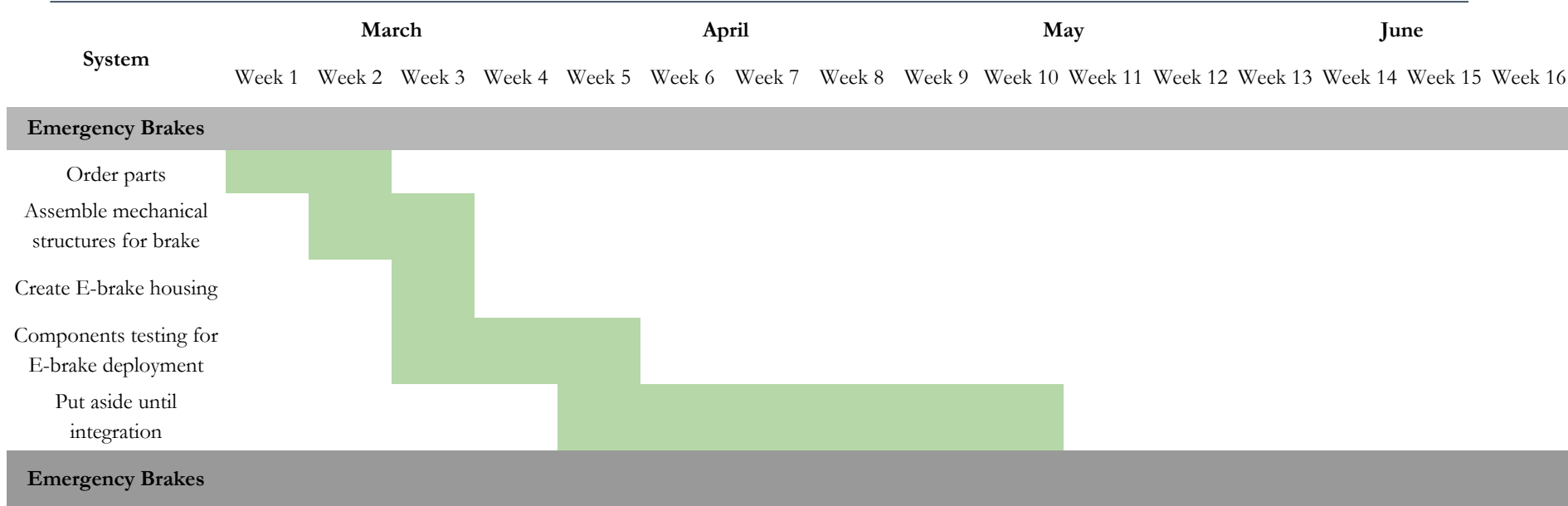
Moving on from a prototype build, to scale up to a fully functional pod, we consider the following features:

- **Levitation re-engagement:** After E-braking, the brake pads can be actively disengaged, thus allowing mechanical rolling to the next induction motor to accelerate the pod once again to levitation speed.
- **Increased spatial dimensions:** With the tube diameter doubling to 12 feet to accommodate a larger pod size, we can update our dimensions to 6 feet tall, 6 feet wide, and 25 feet long. Since the relative capacity of the tube with respect to the pod will remain largely the same, the aerodynamic properties will largely carry over from the current design to the full scale.
- **Cost/mass estimates:** Due to the availability of carbon fiber, the construction of such a pod will not be significantly more than a linear growth with respect to the dimension extensions, but will likely require both another set of four lift arrays and four brake. Rough extrapolation from the current design gives us: \$50,000 and 500 kg for the full scale estimates.
- **Maintenance:** Be able to accommodate passengers and cargo and allow for easy maintenance:
 - Once again, with modularity in mind, the current design uses electropermanent magnets to attach the shell to the chassis. This makes it extremely simple for the pod to be separated and to do maintenance/replacements on the chassis. Other sections that are to be used and anticipated to be broken/replaced can also be attached using these electropermanent magnets.

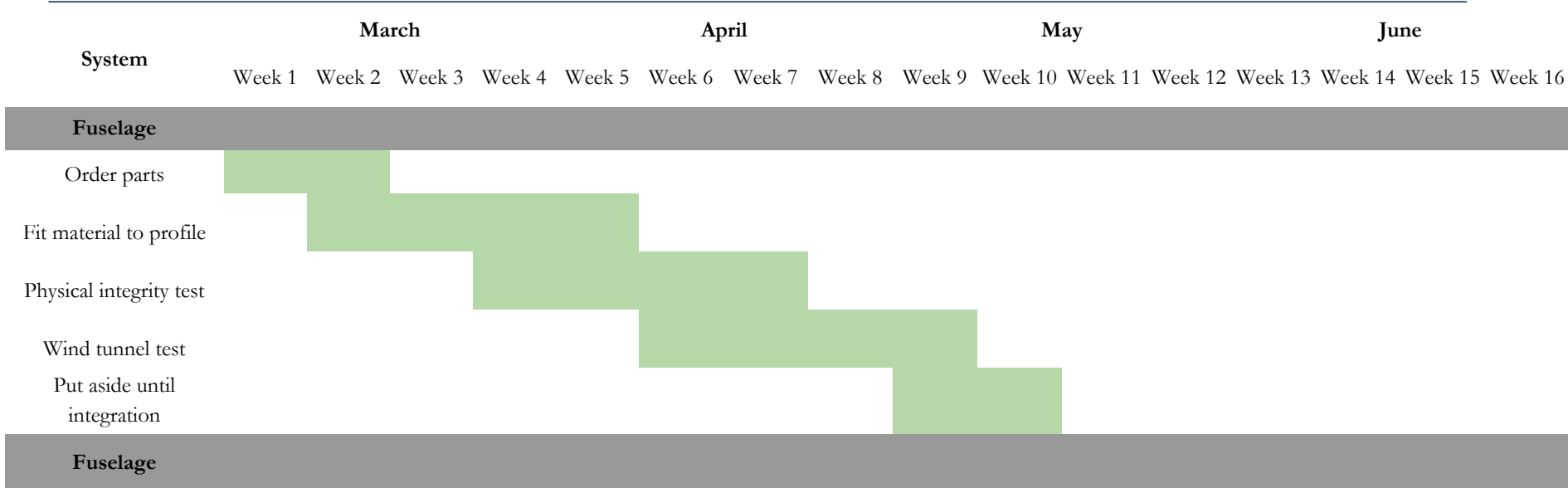
Testing - Production Schedule



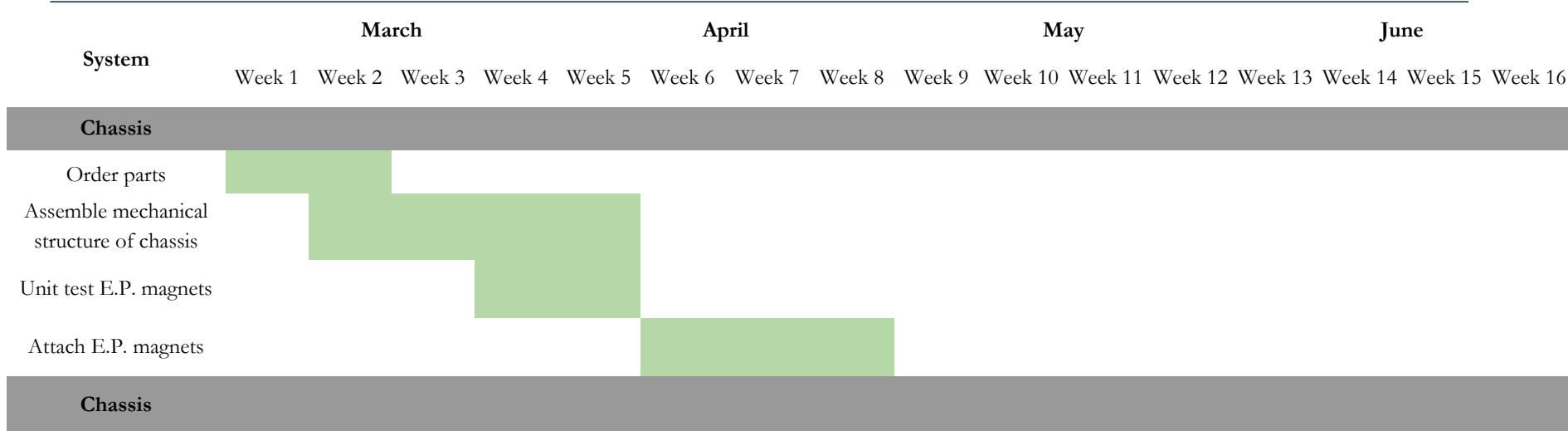
Testing - Production Schedule



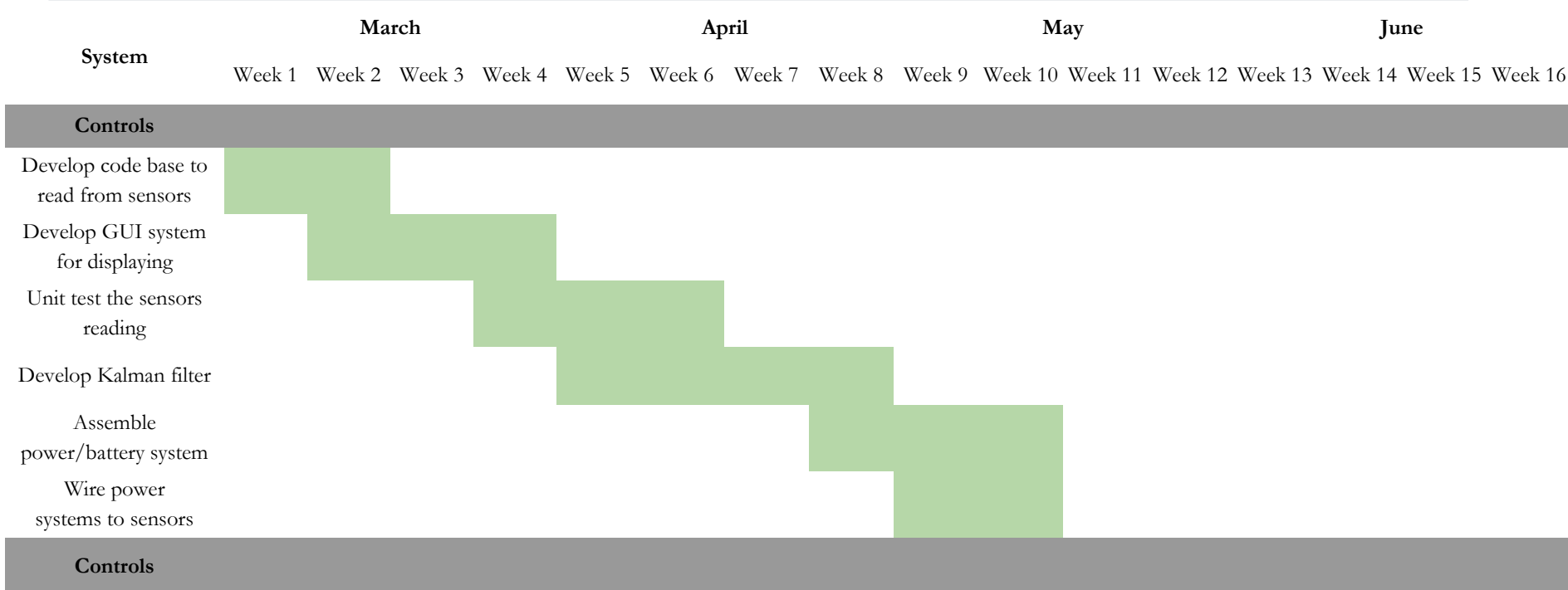
Testing - Production Schedule



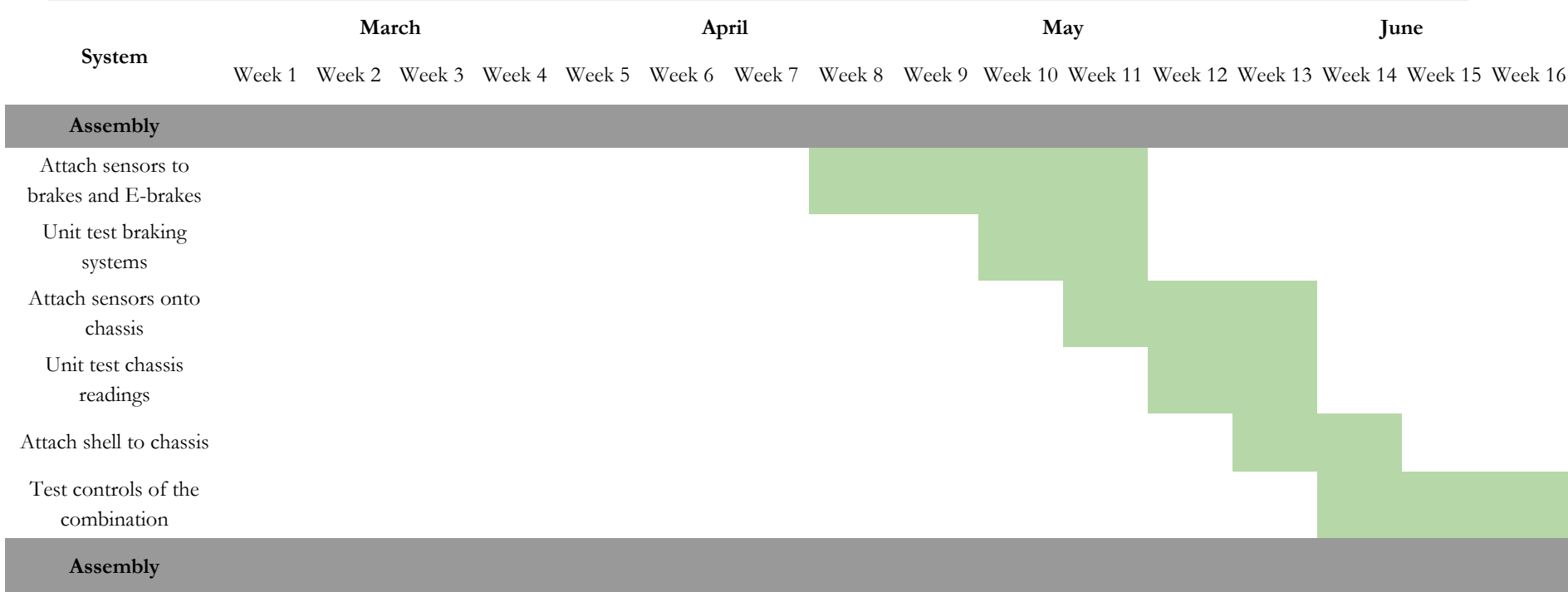
Testing - Production Schedule



Testing - Production Schedule



Testing - Production Schedule

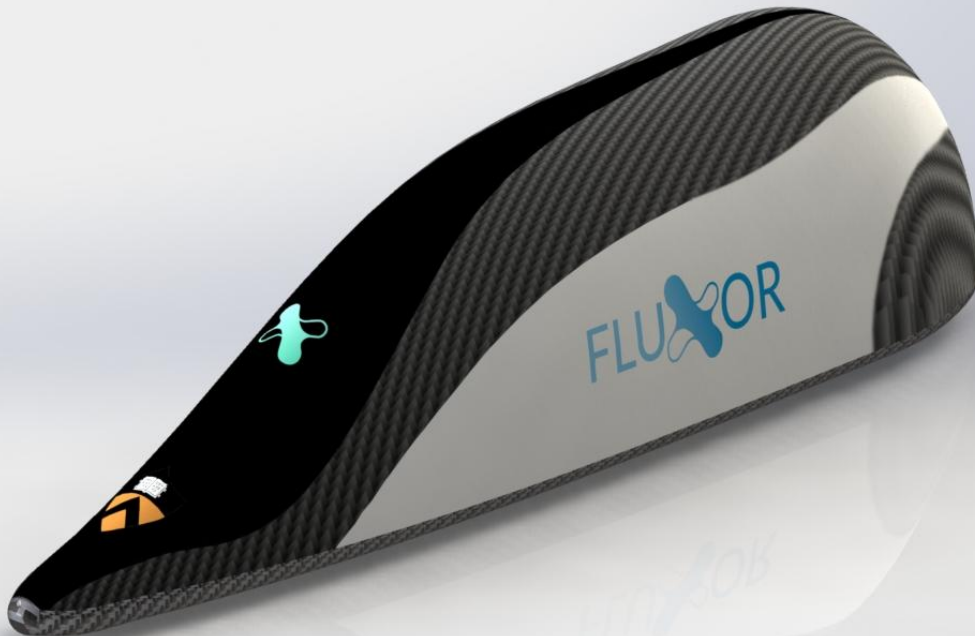


Testing - Competition Weekend II

For the Competition Weekend II setup procedure:

- Pod will be transported on a small cart with caster-wheels at Competition Weekend.
- Cart will include crane attachment points, and sit low enough that the vehicle can slide directly from the cart onto the rail.
- The pod will perform functional tests, which include:
 - Demonstration of power-up by activating battery power
 - Demonstration of chassis/shell lock w/ electropermanent magnets
 - Demonstration of sensors, Raspberry Pi, and communication channels (through GUI readings)
 - Demonstration of linear actuator motors, with test signal from controls system to actuators
 - Demonstration of emergency brake/motors, with a test signal to the ball-pin locks and motors
- When Ready-to-Launch, the pod will rest on its wheels. During launch, it will be accelerated by the pusher, reaching sufficient speeds to lift off from the wheels to be fully suspended by the magnets, on which it hovers for coasting, before braking and landing again on wheeled suspension.
- Refer to Appendix F for full description of pre-launch testing and complete Test Procedures

Appendices



Appendix A: Detailed Mass/Cost Breakdown - Suspension

Part	Model	Quantity	Material	Total Cost (\$)	Unit Weight (kg)	Weight (kg)
Neodymium Magnets	Neodymium 2"x2"x2" Cubes	40	Neodium	4,000.00	.957	38.28
Lift Housing	Custom	4	Aluminum 7075-T6	250	1.5	6.0
Total	N/a	N/a	N/a	4,250	N/a	45.0

*Negligible weight

Appendix A: Detailed Mass/Cost Breakdown - Brakes

Part	Model	Quantity	Material	Total Cost (\$)	Unit Weight (kg)	Weight (kg)
Linear Actuator	Firgelli Classic Linear Actuator	8	Aluminum 7075-T6	640	0.95	7.35
Neodymium Magnets	Neodymium 2"x2"x2" Cubes	40	Neodium	4,000.00	.957	38.28
Brake Housing	Custom	6	Aluminum 7075-T6	400	1.9	11.4
Total	N/a	N/a	N/a	5,040	N/a	57.0

*Negligible weight

Appendix A: Detailed Mass/Cost Breakdown - E-Brake

Part	Model	Quantity	Material	Total Cost (\$)	Unit Weight (kg)	Weight (kg)
E-Brake Frame	Custom	4	Alloy Steel	450	2.6	10.4
Rack Slider	Custom	8	Stainless Steel	480	0.6	4.8
HT-Load Gear	McMaster 5172T360	8	Alloy Steel	640	1.6	12.8
Reinforced Brake Pad	Custom	4	Reinforced Carbon Carbon	300	0.8	3.2
E-Brake Housing	Custom	4	Aluminum 7075-T6	300	1.9	7.6
Three Inch HP Motor	Ampflow E30-400	4	416 Stainless Steel	436	2.2	8.8
Precision Speed Reducer	McMaster 64815K45	4	416 Stainless Steel	500	4	16
				2,462		

Appendix A: Detailed Mass/Cost Breakdown - Chassis

Part	Model	Quantity	Material	Total Cost (\$)	Unit Weight (kg)	Weight (kg)
Electro Permanent Magnets	NicaDrone OpenGrab EPM v3 R5C	14	PCB	826	Negligible	Negligible
2"x2"x12" Aluminum Bars	SQ32	8	Aluminum 6061-T6	1856	25.64	102.56
Wheels	Robart 138B0316-110001M	4	Aluminum 7075-T6	160	0.58	2.32
Rollers	Custom	4	Aluminum 7075-T6	10	.025	0.1
Springs	American Elements AL-M-04-SPG	4	Aluminum 7075-T6	80	0.34	1.36
Total	N/a	N/a	N/a	2932	N/a	106.3

Appendix A: Detailed Mass/Cost Breakdown - Control

Sensor	Model	Number	Total Cost	Unit Weight (g)	Weight (kg)
IR-LED Distance Sensor	GP2Y0A41SK0F	14	192.57	62	.868
Photoelectric Sensor	XUB5BPANM12	4	156.00	3.6	.0144
IMU	KVH 1725	1	1,200	700	.700
Temperature Sensor	Si7050/1/3/4/5-A20	3	3.00	0*	0*
Voltage Sensor	1135_0 Phidgets	3	57.00	1	.003
Total	N/a	N/a	1,610	N/a	1.60

*Negligible weight

Appendix B: Pod Trajectory MatLab Code

Positionprofile.m (code for solving and plotting)

```
% acceleration phase
tspan = linspace(0, 10, 200);
v0 = 0.1;
enddistance = 450;
totaldistance = 1600;
[t, x_accel] = ode45('F', tspan, [0, v0]);
I = find(x_accel(:,1) > enddistance);
i = I(1)-1;
stoptime = t(i);
peakvelocity = x_accel(i,2);
peakdistance = x_accel(i,1);

% coast phase
tspan2 = linspace(stoptime, stoptime + 10, 200);
[t2, x_coast] = ode45('F2', tspan2,
[peakdistance, peakvelocity]);
disp(peakvelocity)
% we begin braking 650 meters before the end
stopdistance = totaldistance - 650;
I2 = find(x_coast(:,1) > stopdistance);
i2 = I2(1)-1;
stopdistance2 = x_coast(i2,1);
stopvelocity = x_coast(i2,2);
```

```
% braking phase
braketime = t2(i2);
tspan3 = linspace(braketime, braketime + 9, 200);
[t3, x_drag] = ode45('F3', tspan3, [stopdistance2,
stopvelocity]);
subplot(2,1,1);
plot(t(1:i), x_accel(1:i,1), t2(1:i2), x_coast(1:i2,1), t3,
x_drag(:,1), 'LineWidth',2);
ylabel('Position (m)');
title('Kinematic profile of pod');
subplot(2,1,2);
plot(t(1:i), x_accel(1:i,2), t2(1:i2), x_coast(1:i2,2), t3,
x_drag(:,2), 'LineWidth',2);
xlabel('Time (s)');
ylabel('Velocity (m/s)');
disp(x_drag(end,1));
```

Appendix B: Pod Trajectory MatLab Code

F.m (pusher phase)

```
function xp=F(t,x)
a = 1.9*9.8;

%We assume that the pusher has a max
acceleration of 1.9 g
podmass = 300;
k = 1;
u_0 = 3.552;
density = 0.00116;
dragcoeff = 0.8;
crosssection = 1.4565;
xp = zeros(2,1);
xp(1) = x(2);
xp(2) = a - 9.8/k / x(2)*(1 -
u_0/sqrt(u_0^2 + x(2)^2)) - ...
0.5 * dragcoeff * density *
crosssection * x(2)^2 / podmass;
```

F2.m (coasting phase)

```
function xp=F2(t,x)
k = 1;
u_0 = 3.552;
podmass = 300;
density = 0.00116;
dragcoeff = 0.8;
crosssection = 1.4565;
xp = zeros(2,1);
xp(1) = x(2);
xp(2) = - 9.8/k / x(2)*(1 -
u_0/sqrt(u_0^2 + x(2)^2)) ...
- 0.5 * dragcoeff * density *
crosssection * x(2)^2/podmass;
```

F3.m (braking phase)

```
function xp=F3(t,x)
k = 1;
k2 = 312;
u_0 = 3.552;
podmass = 300;
density = 0.00116;
dragcoeff = 0.8;
crosssection = 1.4565;
xp = zeros(2,1);
xp(1) = x(2);
xp(2) = - 9.8/k / x(2)*(1 -
u_0/sqrt(u_0^2 + x(2)^2)) ...
- min(k2* x(2)*u_0/(u_0^2 +
x(2)^2),1.8*9.8) ...
- 0.5 * dragcoeff * density *
crosssection * x(2)^2/podmass;
```

Appendix C: Hazard Analysis

The following are potentially “hazardous materials”:

- We will be using three 12 volt batteries in parallel, which may be susceptible to overheating. However, the batteries are reasonably sized and ventilated so overheating should not be an issue.

Appendix D: Detailed Production Schedule

Task Description	Dependencies
1.0 Magnets (Halbach Arrays) System	None
1.1 Design: Choose dimension of magnets and vendor	
1.2 Purchase: Magnets, brake pad material, backing plate, hardware	
1.3 Build: Corner magnet housing (L-mount)	
1.4 Build: Lift magnet housing (rectangular mount)	
1.5 Assemble: Central Halbach array into box housing	

Appendix D: Detailed Production Schedule (cont.)

2.0 E-Brake Assembly	None
2.1 Design: Choose k constant for spring, choose spring size, brake pad material	
2.2 Purchase: Springs (8), tripod extenders, gears, motor, axle, brake pad, controllable ball locks	
2.3 Build: Gear box (assemble gears and mount in housing)	
2.4 Assemble: Springs with brake pad	
2.5 Assemble: Controllable ball locks in tripod extender	
2.6 Assemble: Tripod extender with rack	
2.6 Assemble: Motor with axle and gear box	
2.7 Assemble: Gear box with triboard rack	
2.8 Assemble: Tripod system with housing	
3.0 Lateral Control Assembly	1
3.0 Design: Determine whether the magnets can be smaller than lift magnets	
3.1 Assemble: The assembly of the L-mount housing with the Halbach array	

Appendix D: Detailed Production Schedule (cont.)

4.0 Braking Assembly	1, 3
4.1 Assemble: Actuators with the L-mount housing of the brakes	
4.2 Assemble: Controls to the actuators	
4.3 Assemble: Lift housing to the L-mount brake	
5.0 Wheel Assembly	None
5.1 Purchase: Wheels (4), springs (4), axles (4)	
5.2 Assemble: Wheels with dual axles	
5.3 Assemble: Wheel/axles with springs	

Appendix D: Detailed Production Schedule (cont.)

6.0 Power Supply & Controls

None

6.1 Design: Finalize the Power Equipment Required for Controls

6.2 Purchase: Procure all Power Supply Equipment

6.3 Assemble: Test & Finalize Circuitry

6.4 Assemble: Test & Finalize Housing

6.5 Assemble: Procure Housing and Circuitry

6.6 Assemble: Procure Central Hardware

6.7 Assemble: Code Sensor Fusion and Controls Algorithm

Appendix D: Detailed Production Schedule (cont.)

7.0 Integration

1-6

- 7.1 Assemble: Sensor mounting
- 7.2 Assemble: Frame and shell integration
- 7.3 Testing: Sensor output and Logging test
- 7.4 Assemble: Mount Assembly
- 7.5 Testing: Pressure Test Preparation
- 7.6 Assemble: System in Frame W/ Mounts
- 7.7 Testing: Official LP Test
- 7.8 Testing: Official HP Test
- 7.9 Testing: Static Atmospheric Levitation Tests
- 7.10 Testing: Brake Tests with Depletion
- 7.11 Testing: Side Piston Control Test
- 7.12 Testing: System Troubleshooting

Appendix E: Detailed Testing Program

Functional Tests

1. Functional Test A: demonstration of power-up, by activating the power to the batteries, which will display a light/output to signal running at expected power/voltage.
2. Functional Test B: demonstration of chassis/shell lock, by sending a pulse of power to the electropermanent magnets and ensuring the chassis and shell remain attached prior to being rolled into the tube.
3. Functional Test C: demonstration of sensors, Raspberry Pi, and communication channels operating as expected. The GUI should display reading inputs from all the sensors and with expected values (i.e. no negative values and within expected ranges).
4. Functional Test D: demonstration of the linear actuators in brakes, namely sending a test signal to the linear actuators to ensure they can be deploying and retracted.
5. Functional Test E: demonstration of the emergency brakes and motors, namely sending a test signal to the emergency brake ball locks and motors to see that they are capable of deploying and being retracted.
6. Functional Test F: demonstration that the pod is within 50 ft of the end of the tube and that the velocity reading of the pod is 0 m/s.

Appendix E: Detailed Testing Program (cont.)

Ready-to-Launch Checklist (i.e. things prior to launching pod)

1. On the Staging Area platform, pod will perform Functional Test A, B, and C, which correspond to ensuring the pod can be functionally set up, i.e. chassis and shell could be assembled, continuous communications link is brought up, and sensors being reasonable.
2. Once connected, Gate 1 will then be closed and Functional Test D E will be performed, which essentially ensure that the brakes can properly deploy before running the test.

Ready-to-Remove Checklist

1. Once at pressure, the Pod will perform a Functional Test F in order to verify that it is safe to open Gate 2. If the Pod requires manual movement from the Hyperloop to Exit Area, the test must also verify that the Pod is safe to approach.
2. When the Hyperloop Test Director deems the operation as safe, Gate 2 will be opened.

Appendix E: Detailed Testing Program (cont.)

How pod is moved from Staging Area to HyperLoop

1. Pod will be transported via road to the Hyperloop Staging Area pulled by a road vehicle (i.e. truck) either by the wheels or loaded in a sufficiently large compartment.
2. Pods will be lifted, via a SpaceX provided crane if necessary, onto the Staging Area, an open-air flat surface 20 feet in length.
3. Gate 1 will open after passing functional tests A-C, and the pod will be moved into the Hyperloop using the wheels, since no onboard pod propulsion is used.

How pod is moved from HyperLoop to Exit Area

1. The Pod is responsible for reaching the far end of the Hyperloop, defined as “within 50 feet from Gate 2.”
2. The Hyperloop will then be pressurized.
3. The Pod will then be moved onto the Exit Area, an open-air flat surface 20 feet in length.
4. The Pod will be placed into a safe powered-down “Ready-to-Remove” state, with the electropermanent magnets engaged until the pod is removed from the tube.
5. The Pod will then be removed from the Exit Area via crane.